UCRL 9619

UNIVERSITY OF CALIFORNIA

Ernest O. Lawrence

Radiation Laboratory

ANGULAR DISTRIBUTIONS FROM HEAVY-ION-INDUCED FISSION

BERKELEY, CALIFORNIA

DISCLAIMER

UCRL-9619
UC-4 Chemistry General
TID-4500 (16th Ed.)

UNIVERSITY OF CALIFORNIA
Lawrence Radiation Laboratory
Berkeley, California

Contract No. W-7405-eng-48

ANGULAR DISTRIBUTIONS FROM HEAVY-ION-INDUCED FISSION

Victor E. Viola, Jr.

(Thesis)

March 24, 1961

Printed in USA. Price $2.00. Available from the
Office of Technical Services
U. S. Department of Commerce
Washington 25, D.C.

ANGULAR DISTRIBUTIONS FROM HEAVY-ION-INDUCED FISSION

Contents

ANGULAR DISTRIBUTIONS FROM HEAVY-ION-INDUCED FISSION

Victor E. Viola, Jr.
(Thesis)

Lawrence Radiation Laboratory
University of California
Berkeley, California

March 24, 1961

ABSTRACT

Angular distributions of fission fragments from heavy-ion-induced nuclear reactions were studied. Targets of $_{79}Au^{197}$ and $_{83}Bi^{209}$ were bombarded with $_{6}C^{12}$, $_{7}N^{14}$, and $_{8}O^{16}$ ions at energies of ~5.5 to 10.4 Mev per nucleon. Both targets were also studied with $_{5}B^{11}$ at the maximum energy.

It is observed that the ratio of 0 to 90 deg differential cross sections is much larger for heavy ions than for lighter projectiles. For a given heavy ion, this anisotropy is found to increase with bombarding energy and decrease with the value of Z^2/A of the compound nucleus. There is no distinct evidence for a monotonic relationship between the anisotropy and the mass of the projectile. In this respect, nitrogen is characterized by somewhat lower anisotropies than the other ions.

The data are interpreted within the theoretical framework proposed by Halpern and Strutinski and by Griffin to explain fission-fragment angular distributions at moderate energies. In general, these results can be described in terms of the large angular momenta and excitation energies associated with heavy-ion reactions. It is suggested that, on the average, the number of neutrons that are evaporated before fission increases as the atomic number of the compound nucleus decreases.

I. INTRODUCTION

The recent development of heavy-ion accelerators at Berkeley and at Yale has extended the investigation of nuclear-fission reactions to compound nuclei possessing high spin and excitation energy. Such systems previously were quite difficult to study.

In collisions between heavy ions (A>4) and heavy nuclei, one expects nuclear interactions that are generally classical in character.[1] This simplification arises because the heavy ion, with its greater mass, encounters the target nucleus at a much lower velocity than a lighter projectile of the same energy. Consequently, the probability that the slower particle will be absorbed by the nuclear potential of the target should be enhanced. This process of compound-nucleus formation should increase at the expense of direct interactions between the individual nucleons of the target and projectile. As an additional advantage, the masses and energies involved permit a more distinct separation between compound-nucleus reactions and any direct processes that do occur. Thus, heavy ions should form initial compound nuclei of well-defined mass with large (~100 Mev), but fairly well-known, excitation energies. This is the fundamental information required for the interpretation of any fission process.

Of somewhat greater interest from the standpoint of fission theory is the large orbital angular momentum that is transferred in heavy-ion reactions. For example, 125-Mev carbon ions incident upon gold nuclei produce compound systems with a maximum of 70 units of angular momentum. Such high spin states imply the existence of rather large rotational forces within the excited nucleus. According to the liquid-drop model of fission originally proposed by Bohr and Wheeler[2] and Frankel,[3] the modes of internal energy available for nuclear excitation generate collective oscillations of the nuclear matter. Whenever these oscillations sufficiently distort the nuclear shape, the nucleus becomes unstable and passes over a "saddle point" in the energy of the surface, leading to separation into two or more fragments. It is reasonable

to expect that large rotational forces may significantly affect deformations of the nuclear shape, and subsequently, the mechanics of the fission process itself. This influence should be reflected in both the energetics of the reaction and in the directional behavior of the fission fragments with respect to the axis of rotation.

Swiatecki has extensively investigated many of the deformation shapes leading up to the saddle point.[4] Considerations of a similar nature have been employed by Pik-Pichak and by Hiskes in an attempt to calculate the effect of large angular momenta on rotating liquid drops.[5,6] Both authors conclude that the addition of angular momentum to a nucleus serves to lower the effective potential barrier against fission; hence the probability for fission should increase.

Regarding the directional characteristics anticipated in the division of rotating nuclei, experimental work has shown that fission-fragment angular distributions are related to the spin orientation of the fissioning species. Winhold, Demos, and Halpern were the first to observe anisotropic fission-fragment angular distributions in their studies of photofission.[7] Anisotropy in particle-induced fission was reported soon thereafter in the neutron-fission studies of Brolley et al.,[8,9] and from proton bombardments by Cohen et al.[10] One of the most extensive examinations in the 10 to 40-Mev energy region was by Coffin and Halpern who measured the anisotropies from several heavy targets when fissioned by protons, deuterons, and alpha particles.[11] These and similar experiments are summarized in a number of excellent reviews on the subject of fission.[12-15]

Halpern has summarized the salient features of angular distributions from charged-particle-induced fission as follows:[13]

(a) The fragments come off with greatest probability forward and backward along the beam.

(b) The anisotropy increases in order of the size of the particle inducing fission.

(c) The anisotropy is roughly as large in odd-A targets as in even-even targets.

(d) As the bombarding energy increases, the average anisotropy increases slowly.

(e) The anisotropy in a given fission reaction is largest for the most asymmetric mass ratios.

(f) The anisotropy decreases as the value of the liquid-drop fissionability parameter, Z^2/A, of the compound nucleus increases.

From consideration of the energy and angular-momentum quantum states of stably deformed nuclei, Bohr has proposed a model that is successful in explaining fission-fragment angular distributions at low energies.[16] This approach has been extended to fission at higher energies by Halpern and Strutinski[17] and Griffin.[18] These theories are discussed in Section IVA.

This research was undertaken to determine whether the conclusions applicable to angular distributions at lower energies remain valid for the large excitation energies and angular momenta associated with heavy-ion reactions. That these effects are substantial is evidenced by the highly anisotropic angular distributions recently reported from heavy-ion bombardments.[19-22] The Berkeley Hilac (heavy-ion linear accelerator) provides high beam intensities of B^{11}, C^{12}, N^{14} and O^{16} that are suitable for such studies. The targets chosen were Au^{197} and Bi^{209} which gave compound nuclei ranging in Z from 84 to 91.

A number of factors influenced the selection of these targets. First, both are monoisotopic and easily obtainable in purities that would not require corrections to the data. Second, the heavy-ion fission cross sections for nuclei in this region are quite large,[23] but have sufficiently high fission barriers that the probability for fission from direct interactions should be minimized. Finally, from these two targets a spectrum of compound systems can be formed that spans the radium-actinium region. Fairhall, Neuzil, and Jensen have pointed out that at low energies the fission process apparently undergoes a transition from a mode of primarily asymmetric mass division for $Z \geq 90$ to one that is primarily symmetric below this region.[24] The mass distribution of the

fragments remains one of the unexplained facts of fission. Consequently, it is of interest to see if any observable effects in this Z region might appear at substantial excitation energies.

The experimental objectives of this work, then, are:

(a) to measure angular distributions from specific nuclear species as a function of bombarding energy in order to examine the effects of excitation energy and angular momentum,

(b) to study several related systems in order to provide a comparison of angular distributions from different projectile masses and a series of Z^2/A values for the compound nuclei.

II. EXPERIMENTAL WORK

Angular distributions from fission reactions have been studied by using three methods of fragment detection: (a) direct counting, (b) exposure of photographic emulsions, and (c) radioactivity measurements. Experimentally, each of these techniques utilizes the same basic approach. A thin target of fissionable material is placed centrally in a vacuum chamber of known geometry and bombarded by a well-collimated beam of the desired particles. The resulting fission fragments are detected at a series of angles about the periphery of the chamber—spanning as great a segment between 0 and 180 deg as possible. From the resulting data, one can obtain not only the angular distribution, but also information relating to the fragment kinetic energy and the total fission cross section.

The direct-counting experiments employ gas-scintillation or solid-state detectors. This method provides the greatest potential accuracy because both the differential cross section and the corresponding fragment kinetic-energy spectrum can be measured simultaneously. In the heavy-ion results reported from this technique thus far, only a single element of solid angle at one time has been measured; consequently, the required normalizations introduce a degree of uncertainty into the data. However, recent improvements in this technique have given it a decided advantage over other methods.[25] Emulsion studies provide a measure of the differential cross section for all angles during a single bombardment. In terms of accelerator time and experimental simplicity, this procedure is quite efficient. Because of exposures from reactions other than fission, the data at angles less than 60 deg are subject to considerable uncertainty in these experiments. Also, in high-momentum-transfer reactions, the fission fragments emitted in the extreme backward direction have such low kinetic energies that a detection problem sometimes arises.

The results presented here were obtained by the third technique--that of collecting the fission recoils and measuring their gross radioactivity.

The primary advantage of this approach is that it permits simultaneous measurement of the differential cross section at all angles with a minimum of interference from other nuclear reaction products. On the other hand, this is the least direct of the three methods and its validity depends heavily on the assumption that the observed fission activity represents a true average of the fission process. It is hoped that the following discussion of the experimental work will justify this assumption.

A. Heavy-Ion Beam

The Berkeley Hilac accelerates heavy ions -- primarily boron through neon -- to a constant terminal energy of 10.4 ± 0.2 Mev/nucleon. The nature of these angular-distribution experiments imposes two demands on the beam. First, very thin targets must be used to minimize any stoppage or scattering of the fission fragments within the target material. This factor necessitates a high particle flux in order to produce an observable amount of fission activity. Second, a finely collimated beam is required so that maximum angular resolution is provided. Consequently, the particle flux is substantially reduced, depending upon the success in focusing the beam. Under ordinary conditions, the Hilac beam intensity was sufficient to satisfy these demands. Typical beam levels ranged from 100 to 400 mμamp. In order to build up sufficient radioactivity for good counting statistics, it was found that 500 to 1500 mμamp-hr of total beam were necessary, depending upon the fission cross section at the bombarding energy in question.

Because the Hilac accelerates a fixed-energy beam, it was necessary to use metal degrading foils in order to study reactions at lower energies. Beryllium was found to be the most convenient material because (a) it reduces the loss of beam intensity from scattering reactions, and (b) it minimizes the formation of extraneous radioactive products that could contaminate the fission activity. The thickness of these foils was determined by carefully weighing an accurately known

area of the metal. No range-energy measurements for heavy ions in beryllium are currently available, so that it was necessary to convert the relationships of Northcliffe for heavy ions in aluminum in order to obtain the bombarding energy.[26] This conversion was carried out by multiplying Northcliffe's results by the ratio of the range in beryllium to that in aluminum for protons at the same energy per nucleon as the heavy ion. This ratio has been measured by Sternheimer.[27] It should be noted that the resultant range-energy curves give somewhat higher energies (1 to 3 Mev) below 100 Mev than do the compilations of Hubbard.[28] For this reason the energies stated in Section IIIB are accompanied by the corresponding degrader thicknesses.

It should also be stressed that the energies quoted in this work represent the average projectile energy incident upon the target. In passing through the target, the heavy ions are degraded by 0.5 to 1.0 Mev. The use of degrader foils introduces a spread of approximately 1 to 3 Mev in the energy distribution of the beam particles.

B. Apparatus

The apparatus is shown in Figs. 1 and 2. The chamber was connected to the Hilac tank vacuum which is maintained at a pressure of about 5×10^{-6} mm of Hg. To minimize the danger of contamination from undesirable nuclear reaction products, the degrading foils were placed as far from the target as possible. It was found that at a distance of about 4 to 6 in. in front of the collimation system shown in Fig. 2, a satisfactory balance between extraneous activity and beam loss from scattering was attained.

For a point-focused beam, the collimation system permits a maximum uncertainty of 0.9 deg for any angle. The maximum target area struck by the beam--assuming no substantial enlargement of the beam after passing through the collimators--is 7% of the area of the catchers. Each catcher subtends an angle of 4.6 deg with respect to the target center. When angular-resolution corrections were applied

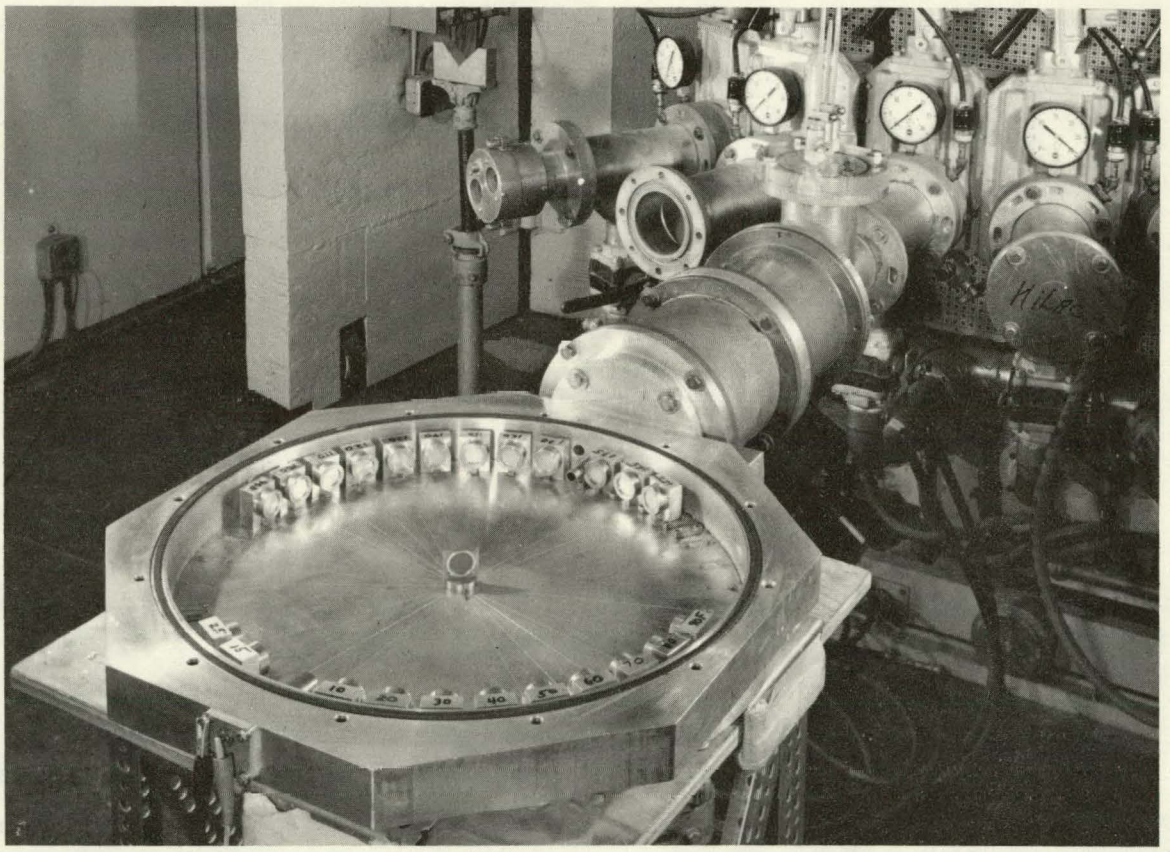

ZN-2748

Fig. 1. Fission-fragment collection chamber.

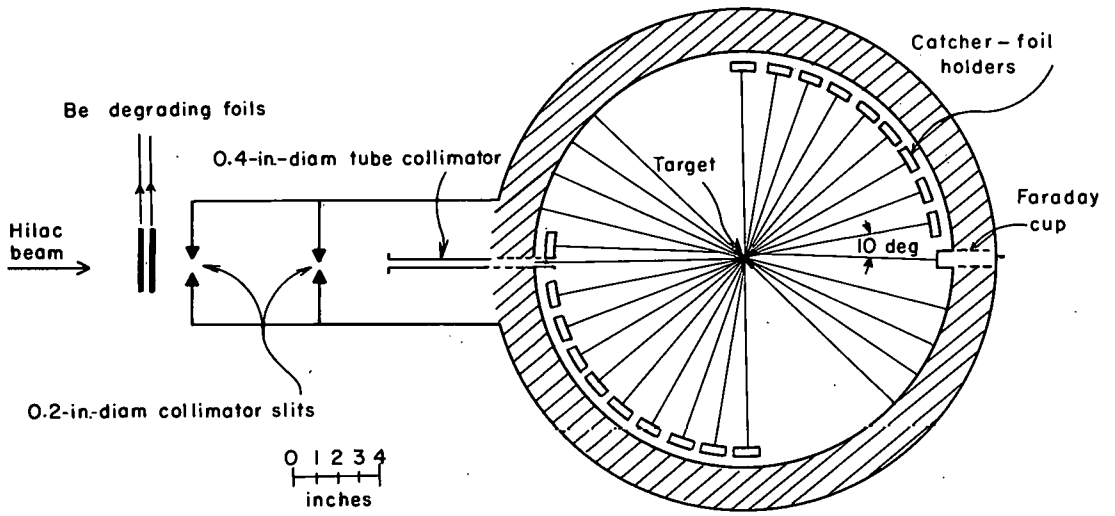

Fig. 2. Top view of the angular-distribution chamber. The chamber is 4 in. deep and 20 in. in diam.

to the data from this arrangement, they were found to be less than 0.5% for the most anisotropic distributions studied. The catcher holders were distributed at 10-deg intervals about the circumference of the chamber. In quadrants I and III with respect to the beam direction, they were placed at 10, 20, ... 170 deg, while in quadrants II and IV positions could be used from 15 to 45 deg and from 145 to 175 deg. A double check on the fission fragments emitted at 90 deg to the beam was provided by placement of catchers on both sides of the target at this angle. The activity of these two catchers was always found to be the same within experimental error.

In some of the early experiments, similar techniques were used to study the angular distributions at angles very near the beam, with better resolution. These experiments were discontinued because it was felt that they did not improve the accuracy of the data sufficiently to warrant the time.

C. Targets

Excellent unsupported targets of gold and bismuth were prepared by vaporizing a thin film of the metal onto a smooth surface.* This film was then removed and mounted on 1-in.-i.d. rings. The thickness of the gold targets ranged from 0.50 to 0.75 mg/cm^2, with an estimated uniformity of better than 5%; that of the bismuth targets was 1.0 mg/cm^2, with a uniformity of about 10%. These uncooled targets survived beam intensities as high as 600 mμamps with little apparent damage from either heat or radiation.

It was assumed that the targets should permit complete recoil escape over a substantial angular range. The bases for this assumption were (a) studies of the recoil ranges of fission fragments,[29] and (b) the effects of target thickness on the measured kinetic energy of the fragments from heavy-ion reactions.[30] Estimates indicate that the target thickness represents less than 10% of the range of the fission fragments emitted along the target normal.

---

*These targets were prepared by Mr. Daniel O'Connell, Vacuum Evaporation Group, Lawrence Radiation Laboratory.

Whenever angular distributions were to be measured with the full-energy beam, two experiments were usually performed--first, with the target at 45 deg to the beam and then with it perpendicular to the beam. This procedure provided a good check on the consistency of the data. In addition it was useful in helping to choose accurate parameters for transformation of the laboratory (lab) data into the center-of-mass (c.m.) system (see Section IIIB and Appendix A). When the data from these two experiments were normalized to one another, excellent agreement was found for all differential cross sections measured at angles of less than 60 deg to the beam. This is shown in Fig. 3 where the ratio of the differential cross section measured with the target perpendicular to the beam to that with the target at 45 deg is plotted versus the lab angle of the catcher. Similar results have been reported by Coffin for alpha-particle-induced fission.[31]

It was a constant feature of comparisons such as Fig. 3 that at angles near 70 and 110 deg a value of about 1.05 ± 0.04 was obtained for this cross-section ratio. One expects that the ordinate of these plots should never exceed unity. A possible explanation could be that particles emitted near 90 deg to the target normal are highly scattered; hence, the activity of adjacent points might be enhanced. However, Coffin has performed calculations that indicate the fragments should not be appreciably scattered until very near the end of their range. For this reason, thin cover foils had been placed over the fission product catchers to eliminate this undesirable activity. The magnitude of the effect is small, though, and in view of the fact that it did not alter the over-all angular-distribution data, it was not investigated further.

It was subsequently assumed that a single experiment with the target oriented at 45 deg should be sufficient to determine the angular distributions for lower-energy bombardments. Data were taken at angles up to 70 deg, but the errors from all data taken at angles of greater than 55 deg to the target normal were weighted more heavily.

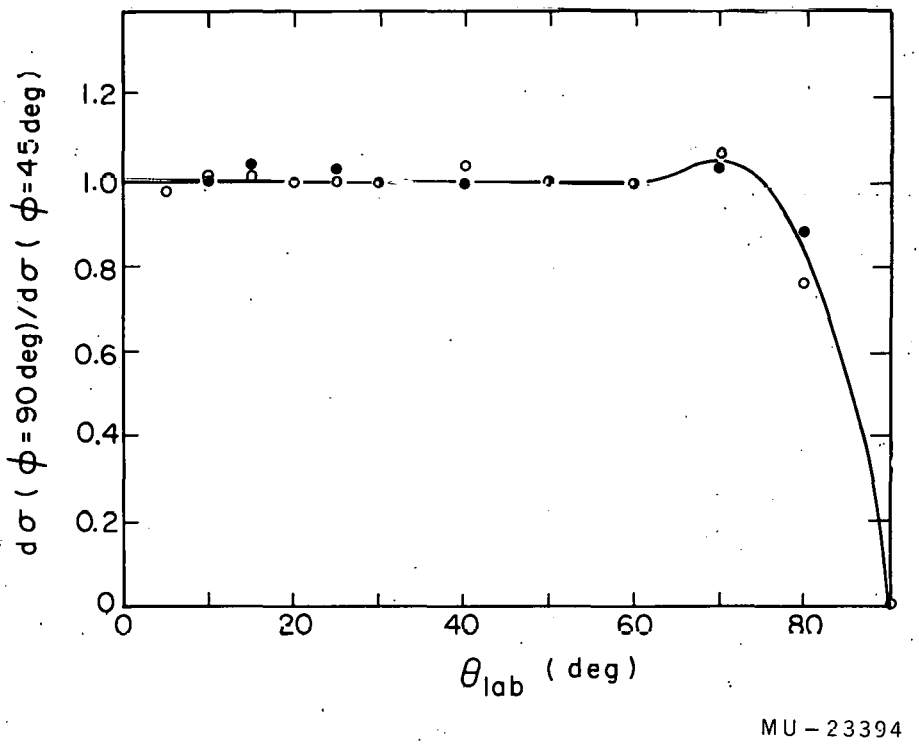

Fig. 3. Ratio of the differential cross section obtained with target angle, ϕ, at 90 deg to the beam to that at 45 deg as a function of the catcher angle. (●--catcher angle θ; O--catcher angle $\pi-\theta$; ◑--catcher angles θ and $\pi-\theta$). Errors are about 4% in all cases.

D. Recoil-Collection Techniques

For these experiments to yield accurate angular-distribution data, the fission fragments must possess ranges that are distinct from those of other reaction products. Concurrent work involving recoil studies of heavy-ion reactions provided much valuable information for the initial phases of this work.[29,32,33] Figure 4 shows four differential range measurements of the reaction products at selected angles. In Fig. 4(a), full-energy O^{16} is incident upon Bi^{209} with the target at 45 deg. In Fig. 4(b), (c), and (d), Au^{197} was bombarded with C^{12} at 112.1 Mev, with the target perpendicular to the beam. At each angle a stack of 0.92 mg/cm^2 Mylar discs was used to collect the recoil activity. This information was later used as the basis for selection of proper catcher thicknesses at other angles.

Figure 4(a) represents the general features of these differential range plots at the most perverse angle studied--10 deg. The activity in the initial catcher was assumed to be due to spallation products, as indicated by the range studies of Alexander and Winsberg.[32] This catcher usually contained 5 to 10 times as much activity as any other. In most cases of bombardment with full energy beams, the second catcher foil had little activity; thus a distinct separation between the spallation products and longer-ranged activities was furnished. At a range of 2 to 4 mg/cm^2 of Mylar, a second peak of activity was observed. This was known to contain the fission products as determined from the radiochemical separations by Blann[34] and also by this experimenter. Finally, the long tail of activity which follows the fission peak is attributed to activation of the catchers induced by scattered beam particles. Aluminum foils, which were used in the early work, proved to yield a greater amount of this latter activity with respect to the fission peak. Therefore, Mylar was selected as the catching material in subsequent work.

A comparison of Figs 4(b), (c), and (d) demonstrates the decrease in the activity as a function of the angle that one expects for

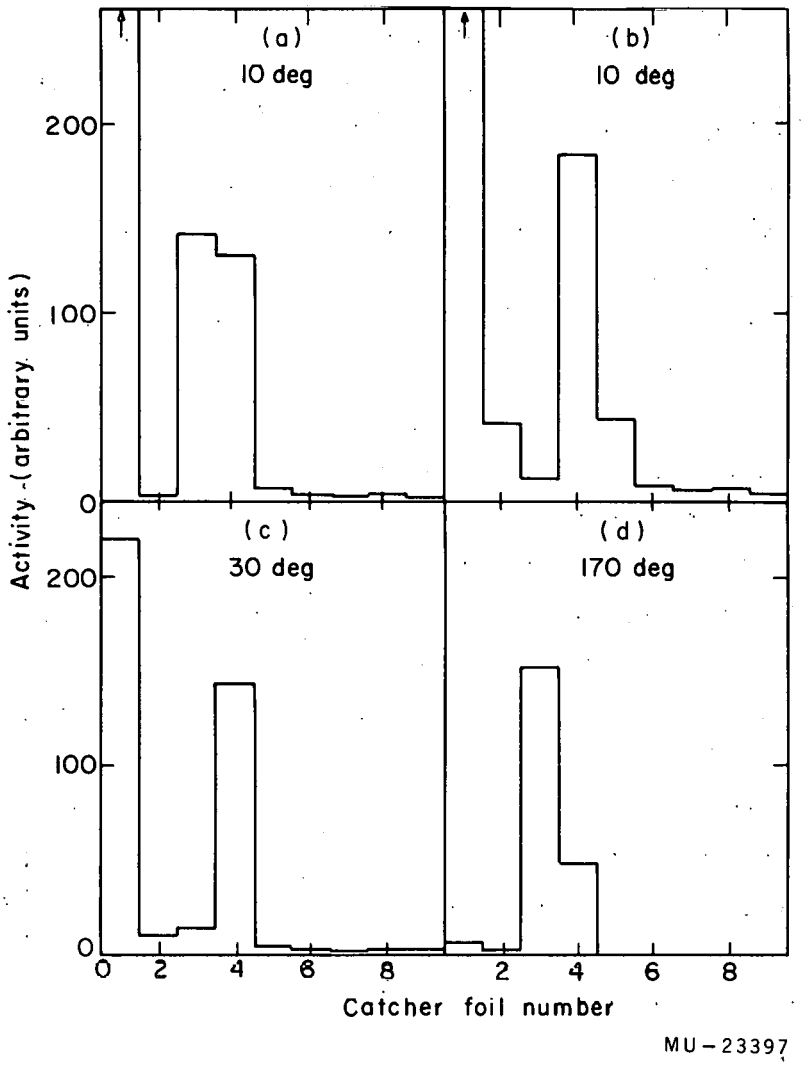

Fig. 4. Differential range results for radioactivity observed from bombardments of: (a) 166.1-Mev O^{16} on Bi^{209} at 10 deg, and 112.1-Mev C^{12} on Au^{197} at (b) 10 deg, (c) 30 deg, and (d) 170 deg. Each catcher thickness is 0.92 mg/cm^2.

spallation products and activation from scattered beam. Figure 4(d) is typical of the differential range curves observed from 40 to 175 deg. Taking advantage of this information, two basic arrangements of catchers were employed. These are shown in Fig. 5. From 40 to 175 deg, a cover of 0.92 mg/cm^2 was placed over two 3.30 mg/cm^2 Mylar discs. The first 3.30 mg/cm^2 disc served as a catcher for the fission recoils and the second was used as a blank. (With aluminum foils, the cover thickness was 1.1 mg/cm^2 and that of the catchers was 4.70 mg/cm^2.) At no time was any activity observed in the blank. When bombarding with nitrogen and oxygen, there was increased danger that the covers might stop some of the fission recoils emitted in the extreme backward directions. This result could arise because of the large forward component of momentum in the lab system for the fissioning nucleus. As a precaution, 0.31 mg/cm^2 Mylar* was used as the cover from 155 to 175 deg in many of these experiments. However, identical experiments--except for these two different cover thicknesses--showed no discrepancy between one another.

The second catcher arrangement, for angles between 10 and 30 deg, exploited the differential-range technique. Usually, 10 to 12 0.92 mg/cm^2 Mylar discs served as catchers. It was felt that this procedure provided better estimates of errors and a more reliable correction for catcher activation. The major source of uncertainty encountered at these angles stemmed from the activity that is seen in the second catcher of Fig. 4(b). Whenever this was present, the clear-cut distinction between the fission and spallation products was reduced. This activity exhibited gross decay characteristics different from those of the fission recoils, but was too long in range to be due to spallation products. At first, it was suggested that some unexpected nuclear reaction product might be emerging from the target. However, the appearance fluctuated from one bombardment to another and showed

*I am indebted to H. E. Knipmeyer of the film department of E. I. DuPont de Nemours and Co., Wilmington, Delaware, for furnishing me with this special film.

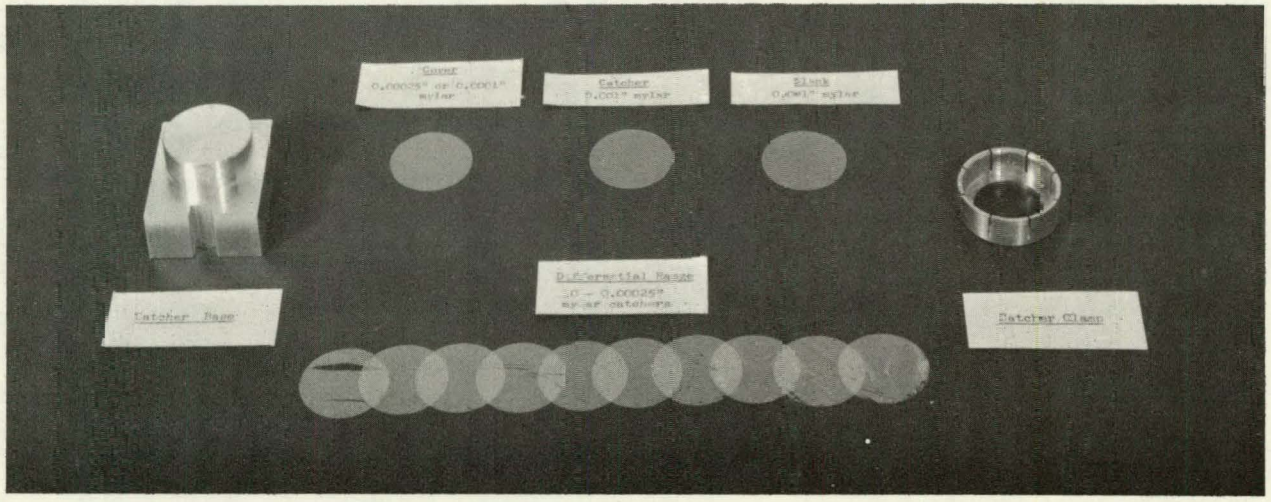

ZN-2749

Fig. 5. Catcher-holder arrangement.

no consistent behavior as a function of particle, energy, or target. The only two variables that could be correlated with the activity were (a) the amount of degrading foil present, and (b) the success in focusing the beam. Consequently, it was presumed that this activity most probably originates in the degraders and collimators and is subsequently scattered from the end of the collimator tube or the target.

It should be added that the above effect is enhanced markedly when aluminum is used as the degrader. Altman has found that heavy ions incident upon aluminum produce P^{32} and Na^{24} with cross sections of tens of millibarns.[35] The angular distribution of these products is strongly peaked in the forward direction with ranges sufficient to penetrate the first Mylar disc. It is quite likely that products of a similar nature could be the source of this spurious activity.

E. Fission-Recoil Radioactivity

1. Detection Technique

At the end of a bombardment, the catchers were rapidly removed from the collection chamber and mounted on standard counting discs. Initial counts usually began within 10 min after the bombardment had ceased. The catcher activity was detected at 32 counting stations equipped with Geiger-Mueller tubes and arranged for simultaneous counting of the samples. The register signal from each of the standard scaling units of the counter was fed into a converting system where the signal voltage was modified to a distinct pulse height. The emergent graded pulses were then recorded on corresponding channels of a Penco 100-channel analyzer. The samples were counted until good statistics were obtained, and then rotated systematically to other counters. This procedure was repeated throughout the counting period in order to minimize errors resulting from any variation in counter efficiencies and geometries. To further insure consistency of the counting rates, a beta standard was also circuited through the system to establish a basis for normalization of the counting rates.

2. Decay Characteristics

Initially, careful experiments were carried out to make certain that the fission-product decay was composed of many components and that the angular distributions did not change with time. In previous studies by Coffin and Halpern, this behavior was confirmed.[11] In this work we are concerned with much more anisotropic distributions and lighter fissioning systems, so that a different behavior might have been observed.

In order to test this possibility, a prolonged bombardment of gold with 125-Mev C^{12} was performed. The recoil catchers were not rotated through the counters, in order to provide maximum consistency for the decay at a given angle. The results at three widely separated angles are shown in the decay curves of Fig. 6, which also includes the ratios of the various activities as a function of time. The decay is certainly composed of a large number of components, and there is little fluctuation in the activity ratios with time. Following the decay over a period of two days showed no noticeable change in these observations. Consequently, it was concluded that the experimental technique should give an accurate description of angular distributions from heavy-ion-induced fission reactions.

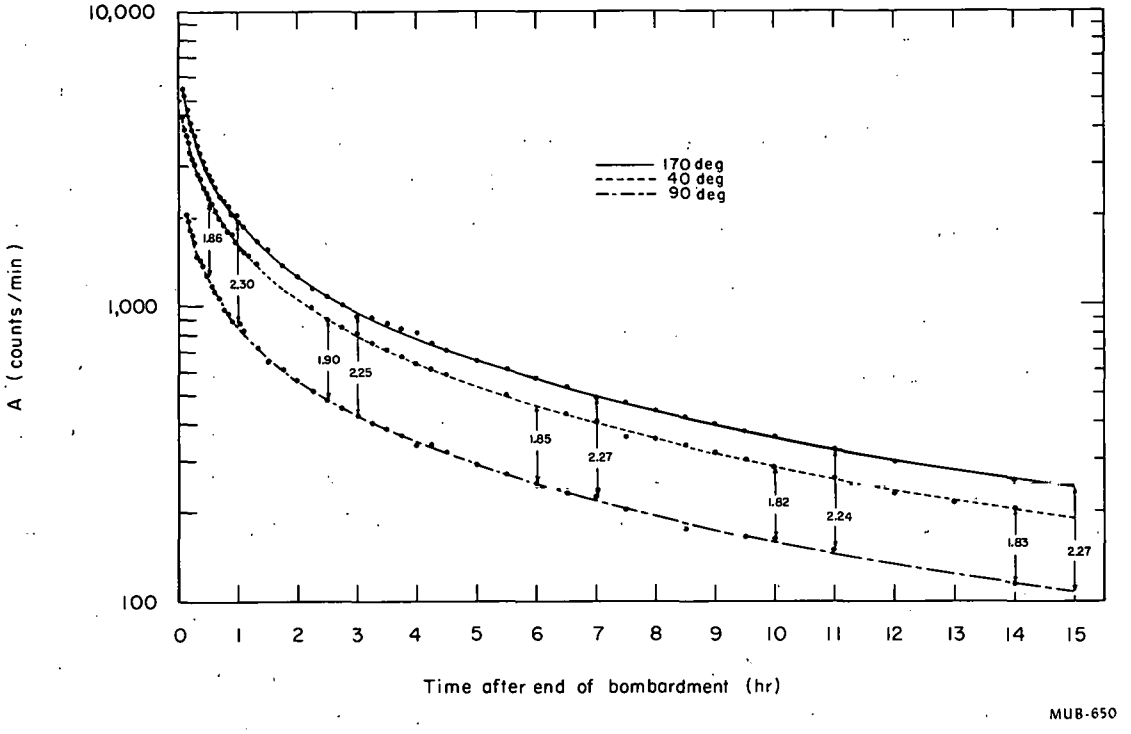

Fig. 6. Gross fission-fragment beta activity as a function of time. Limits of error on points are < 2%.

III. TREATMENT OF DATA AND EXPERIMENTAL RESULTS

A. Laboratory Angular Distributions

To obtain the lab angular distributions, the initial data from each experiment was processed as follows. The counting rates were first corrected for background and for coincidence losses, and then normalized to one another from the counter standardization. The decay of each sample was plotted as previously shown in Fig. 6 to give a family of decay curves corresponding to the angular distribution. Because of the double check at 90 deg, this decay curve was arbitrarily assigned a differential cross section of unity in the lab system. Hence, the relative differential cross section, $d\sigma(\theta)/d\omega$, was obtained by dividing the catcher activity at the angle θ by that at 90 deg at a given time. In order to obtain the differential cross sections between 10 and 30 deg, the fission-product decay was summed from the differential range portion of the experiment and appropriate subtractions for induced activity were performed. Placement of circular discs on a circumference about the target removes the necessity of any solid angle corrections to the data.

For each experiment a series of angular distributions corresponding to a fixed fraction of decay were calculated. Averaging these relative differential cross sections over the entire decay period gave the final lab angular distribution. Figures 7 through 14 present these results for B^{11}, C^{12}, N^{14}, and O^{16} incident upon Au^{197} and Bi^{209} targets, respectively. For all bombarding ions except B^{11}, the projectile energies were varied from the maximum Hilac energy to as near the Coulomb barrier as experimentally feasible. Because of the rapid decrease in the fission cross section as a function of energy near the Coulomb barrier, experiments at the lowest energy are subject to increased error due to low counting rates.

Several sources contribute to the limits of error. The primary uncertainty in the over-all distributions stems from the standard deviation calculated from the various angular distributions as a function of

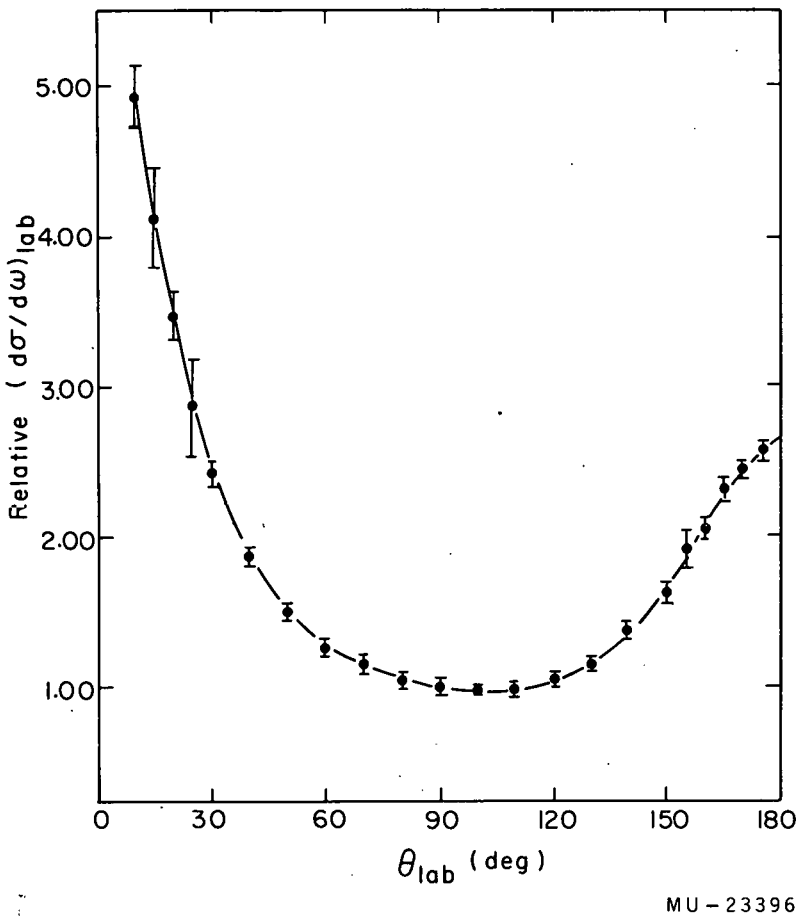

Fig. 7. Laboratory angular distribution from Au^{197} bombarded with B^{11} at 114.3 Mev. The errors represent standard deviations. The differential cross section at 90 deg is unity.

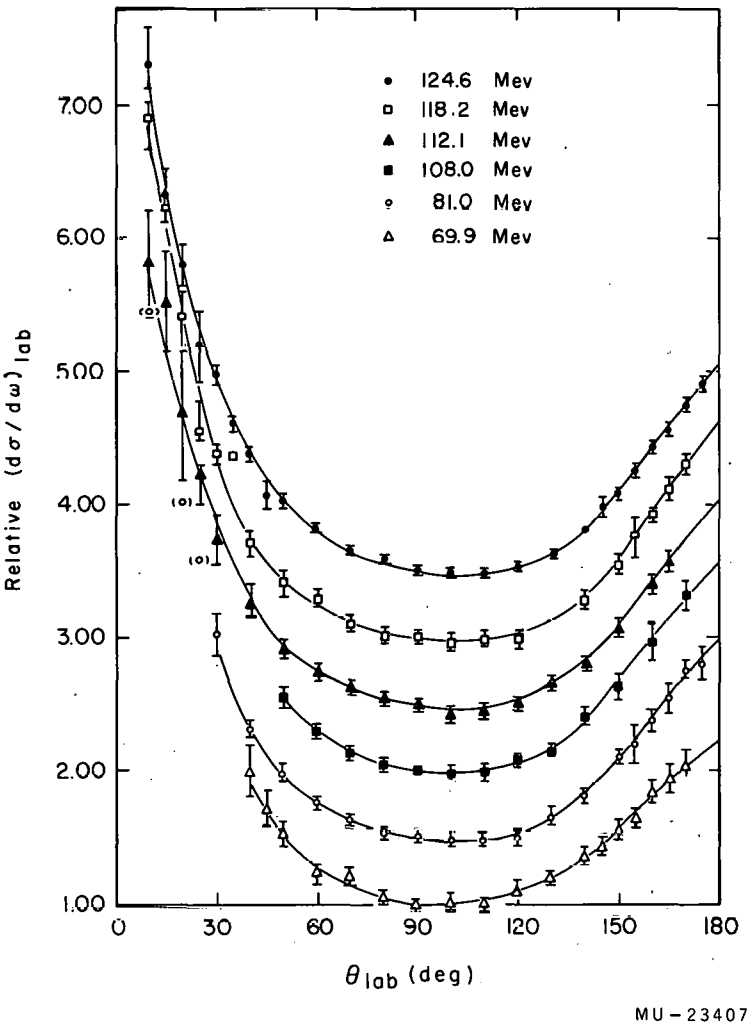

Fig. 8. Laboratory angular distributions from Au^{197} bombarded with C^{12}. The errors represent standard deviations. The differential cross section at 90 deg is unity.

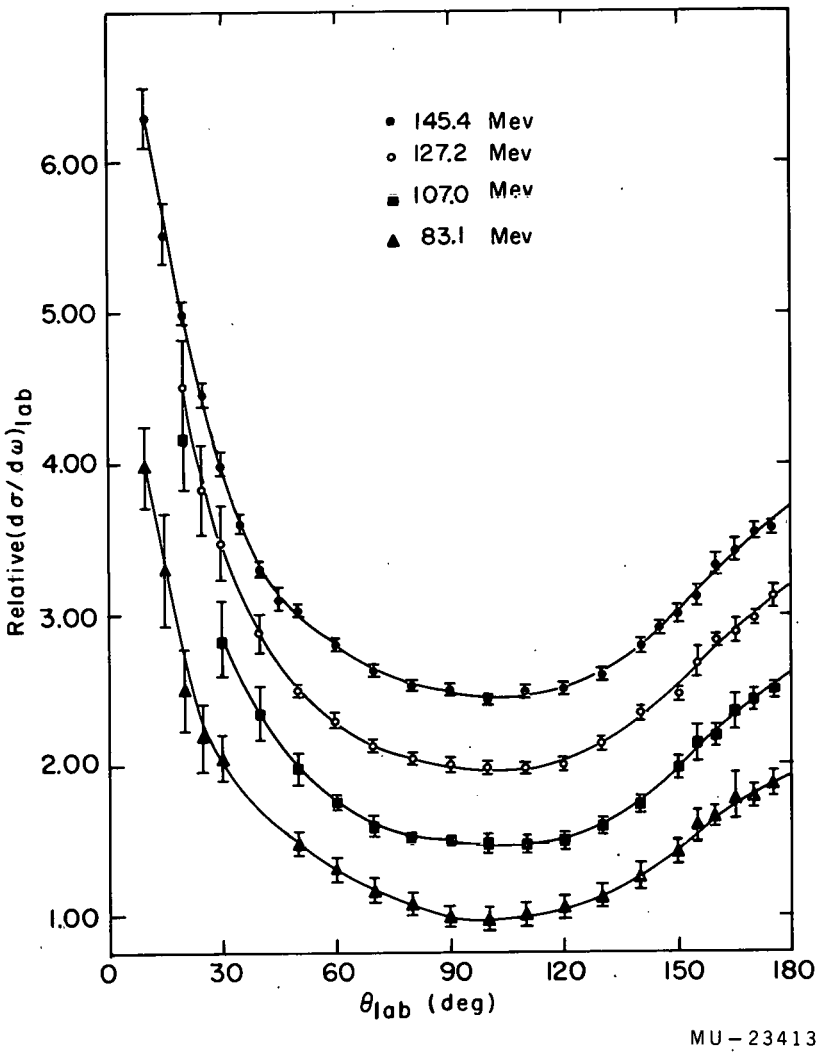

Fig. 9. Laboratory angular distributions from Au^{197} bombarded with N^{14}. The errors represent standard deviations. The differential cross section at 90 deg is unity.

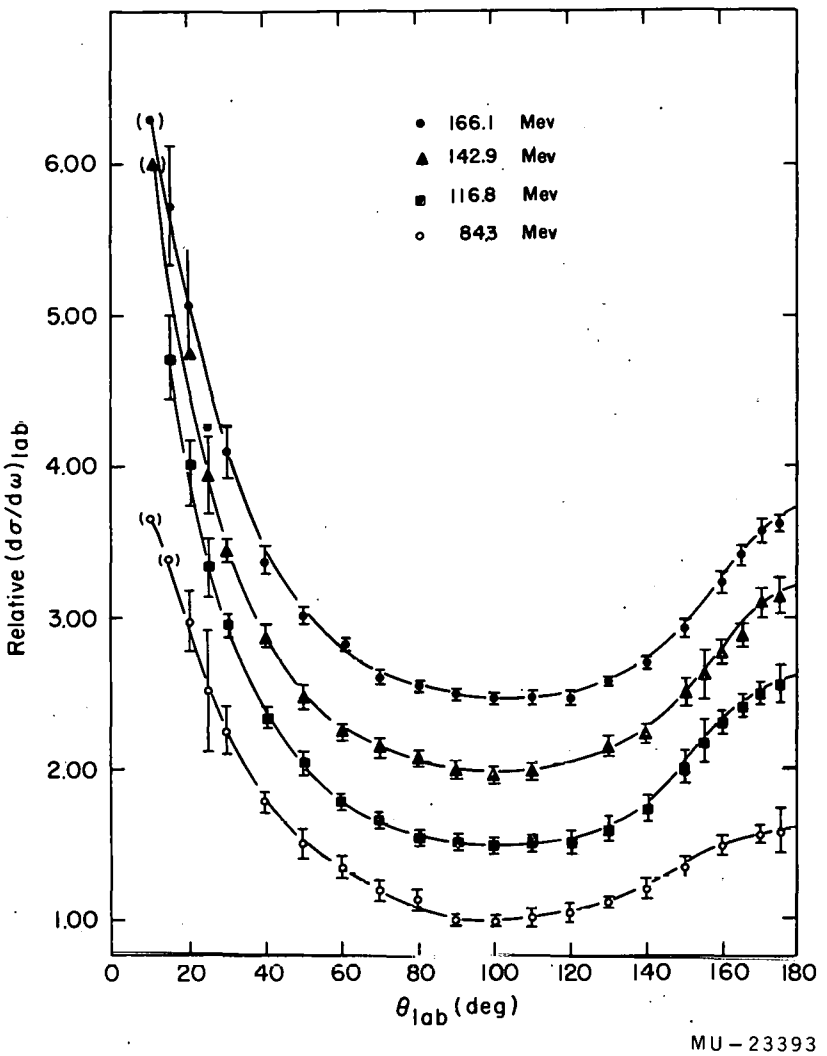

Fig. 10. Laboratory angular distributions from Au^{197} bombarded with O^{16}. The errors represent standard deviations. The differential cross section at 90 deg is unity.

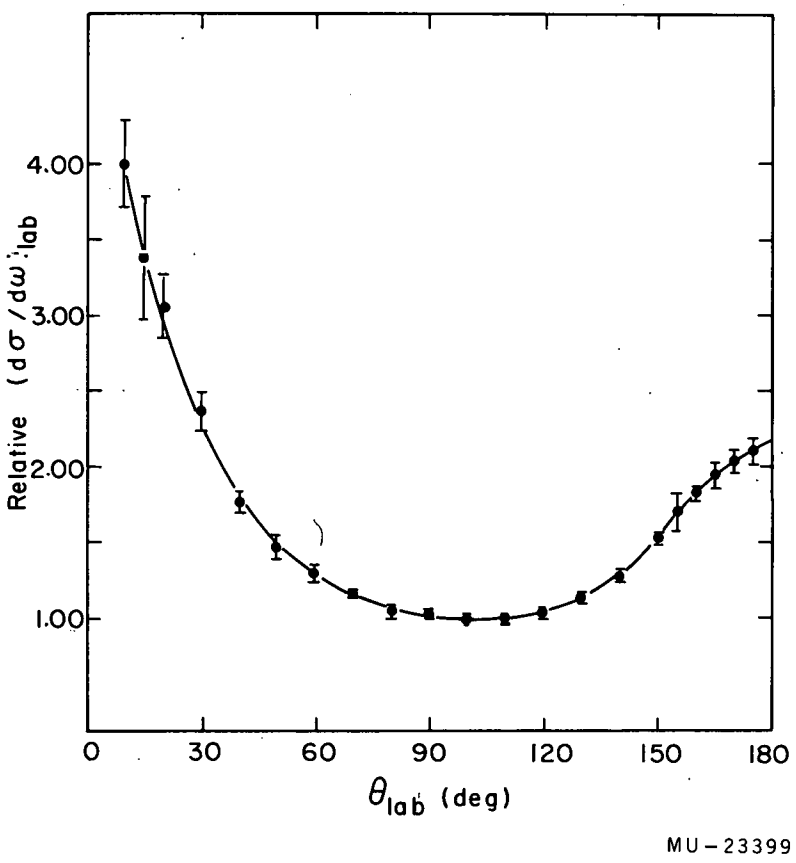

Fig. 11. Laboratory angular distributions from Bi^{209} bombarded with B^{11}. The errors represent standard deviations. The differential cross section at 90 deg is unity.

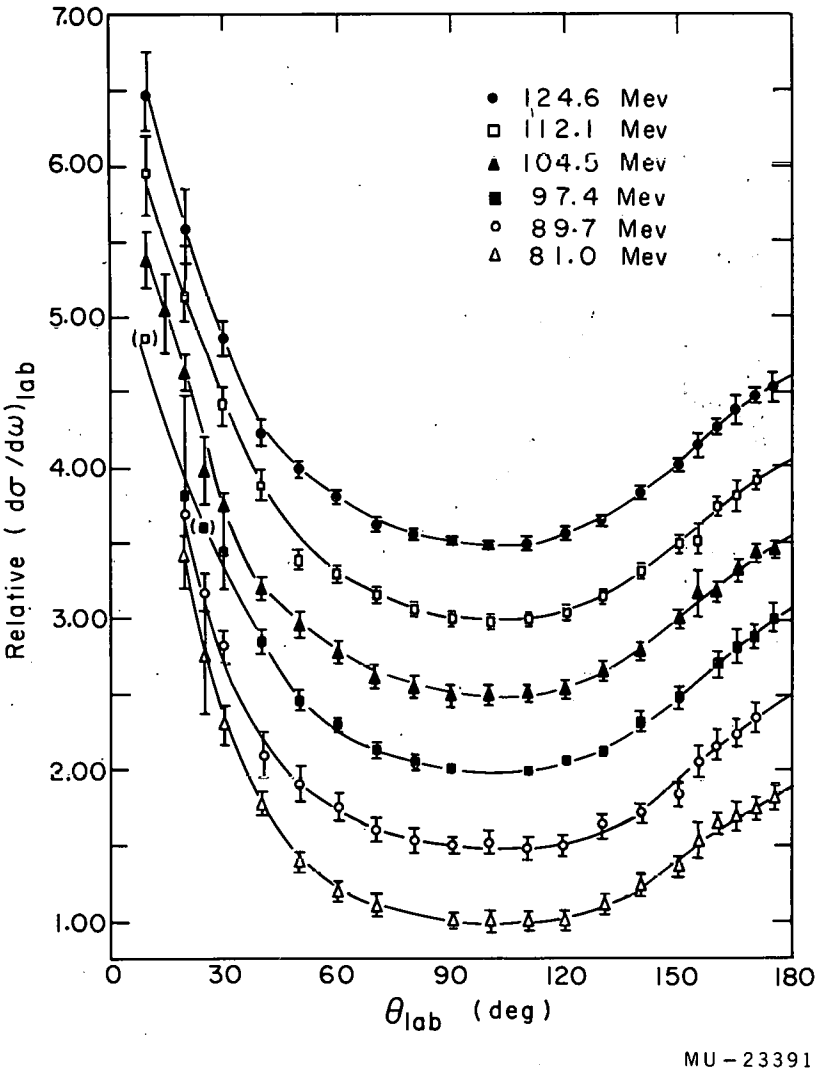

Fig. 12. Laboratory angular distributions from Bi^{209} bombarded with C^{12}. The errors represent standard deviations. The differential cross section at 90 deg is unitv.

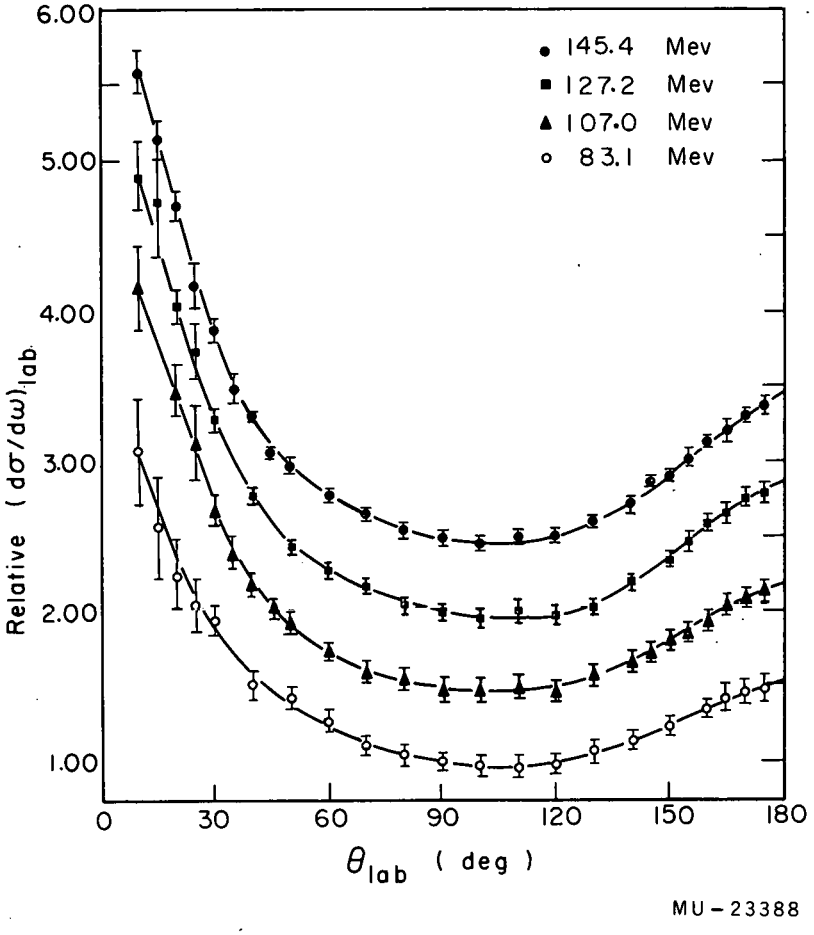

Fig. 13. Laboratory angular distributions from Bi^{209} bombarded with N^{14}. The errors represent standard deviations. The differential cross section at 90 deg is unity.

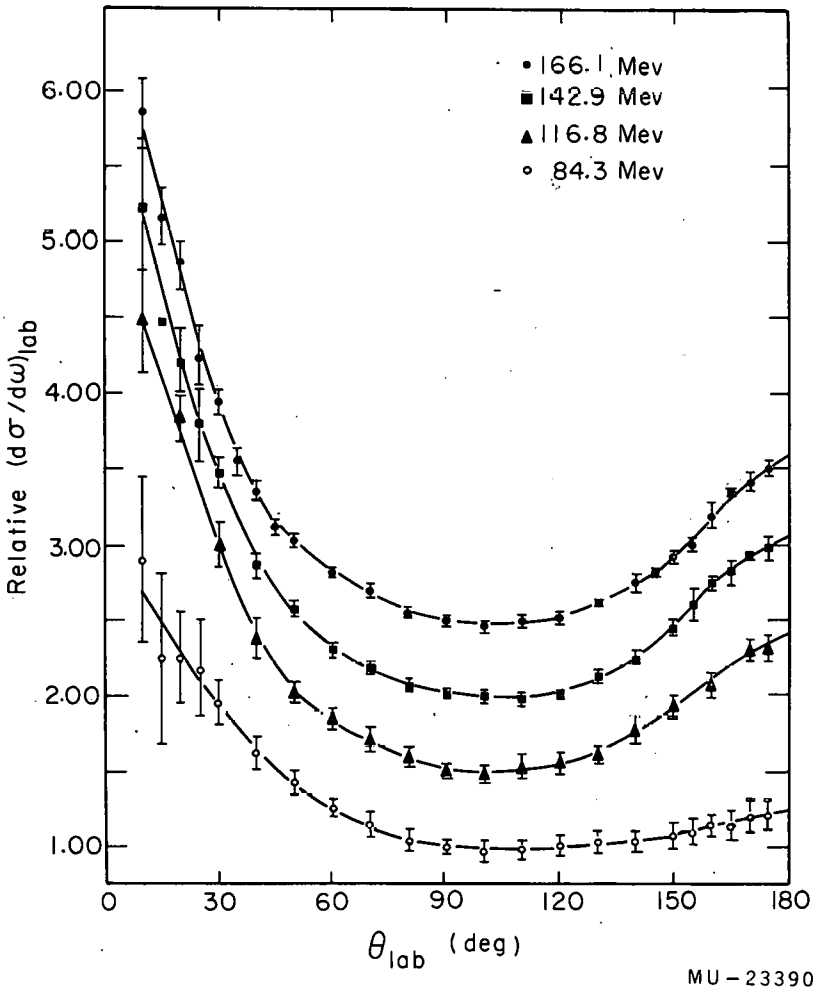

Fig. 14. Laboratory angular distributions from Bi^{209} bombarded with O^{16}. The errors represent standard deviations. The differential cross section at 90 deg is unity.

time. It should be pointed out that the decay curves were not, in general, as consistent as those shown in Fig. 6 because of the rotation of the samples through the counting system. Differences in counter geometry and efficiency, as well as high backgrounds created by the rf field of the Hilac, contribute to the fluctuations. Thus, this error includes both inconsistencies in the detection system and, to a lesser extent, possible variations in the angular distributions with time. In all cases counting statistics were known to better than 2%. At small forward angles the largest source of error originates in the extraneous activity discussed in Section IID. In calculating these differential cross sections, it was assumed that all activity with a range less than 1.8 mg/cm^2 of Mylar was not due to fission recoils. The fraction of the extraneous activity to the total-fission activity at a specific angle was used to compute the error contribution. Whenever this ratio was greater than 15%, the data point was rejected.

Comparison of the lab angular distributions shows the following correlations:

(a) The lab backward anisotropy--i.e., the extrapolated ratio of $d\sigma(180\ \text{deg})/d\sigma(90\ \text{deg})$--behaves for both targets according to the trend: boron > carbon > nitrogen $\simeq$ oxygen.

(b) For a given heavy ion, the anisotropy is greater with a gold target than with a bismuth target at the same incident energy.

(c) For a given bombarding ion and target, the lab angular distributions change very slightly with energy until one approaches within 20 to 30 Mev of the Coulomb barrier. Below this point, the anisotropy decreases much more rapidly, e.g., as in Fig. 14, which shows the angular distributions of fission fragments from O^{16} bombardment of Bi^{209}.

B. Center-of-Mass Transformations

To compare experiment with theory, we must transform the lab angular distributions into the more meaningful c.m. system. These two coordinate systems are related by the vector diagram

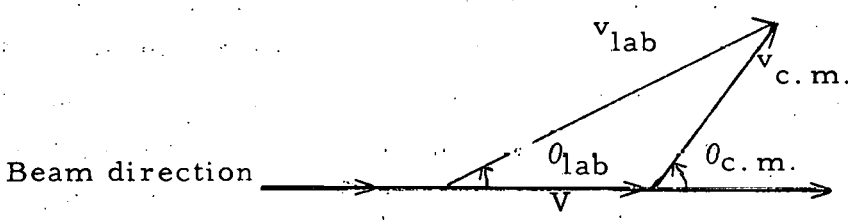

where v_{lab} and θ_{lab} are the velocity and angle to the beam direction, respectively, of a fission fragment in the lab system; $v_{c.m.}$ and $\theta_{c.m.}$ are the same quantities in the c.m. system, and V is the velocity of the center of mass.[36] In this picture, we assume that the incident heavy ion transfers all of its momentum to the compound nucleus, and that the disorientation of the recoils caused by light-particle evaporation from any of the nuclei is negligible. The large mass of these systems makes this assumption valid within a few percent. The angular correspondence between these two systems is given by

$$\tan \theta_{c.m.} = \frac{\sin \theta_{lab}}{\eta + \cos \theta_{lab}} , \qquad (1)$$

where $\eta = V/v_{c.m.}$. The change in solid angle resulting from this angular correction requires that the differential cross sections be corrected by

$$(d\sigma/d\omega)_{c.m.} = G(\eta, \theta)(d\sigma/d\omega)_{lab}, \qquad (2)$$

where

$$G(\eta, \theta) = \frac{(1 - \eta^2 \sin^2 \theta_{lab})^{1/2}}{\left[\eta \cos \theta_{lab} + (1 - \eta^2 \sin^2 \theta_{lab})^{1/2}\right]^2} . \qquad (3)$$

Thus, if the quantity η is known, the c.m. transformation can be performed.

Although a single value of η cannot be applied rigorously to a manifold nuclear reaction such as fission, an average quantity that applies to the gross process can be approximated in several ways:
(a) If one assumes that only binary events occur in these fission reactions, the angular distribution must be symmetric about 90 deg in the c.m. system. By trial-and-error transformations, $\bar{\eta}$ can be determined from the value that yields the most symmetric distribution.
(b) One can also obtain $\bar{\eta}$ from the lab angular distribution by plotting the ratio of the forward differential cross section at an angle θ to that at $(\pi-\theta)$ versus the angle θ. If one extrapolates this plot to $\theta = 0$ deg, then from Eqs. (2) and (3) we have

$$\bar{\eta} = \frac{x^{1/2}-1}{x^{1/2}+1} \quad , \tag{4}$$

where x is $d\sigma(0 \text{ deg})/d\sigma(180 \text{ deg})$ in the lab system.
(c) If there is complete momentum transfer in the reaction, $\bar{\eta}$ can be calculated from the formula

$$\bar{\eta}^2 = \frac{M_p E_p M_f}{M_{CN}^2 \bar{E}_{c.m.}} \quad , \tag{5}$$

where M_p and E_p are the mass and lab kinetic energy, respectively, for the heavy ion; M_f and $\bar{E}_{c.m.}$ are the mass and c.m. kinetic energy of the average fission fragment, and M_{CN} is the mass of the fissioning compound nucleus. Measured values of $\bar{E}_{c.m.}$ near 75±3 Mev have been reported for heavy ions on gold and 80±3 Mev for heavy ions on bismuth.[19,20] These values are roughly independent of the bombarding energy. As a first-order approach, one can assume that M_f is one half M_{CN}. This calculation is treated in Appendix A.

The $\bar{\eta}$ values determined by each of these three methods are listed in Table I along with corresponding bombarding energies and degrader thicknesses. Selection of $\bar{\eta}$ for the final c.m. transformations was based on the first method. Radiochemical studies by Haines, which sought specifically to determine the degree of tripartition in the reaction $U^{238}(C^{12}, f)$, indicate that only binary fission should be observed in the systems with which we are concerned here.[37] Therefore, it was decided that symmetry about 90 deg in the c.m. system should be the most reliable basis for transforming the data consistently. These trial-and-error transformations were performed on the IBM-650. When the second method of fixing $\bar{\eta}$ was used, it was difficult to extrapolate the plots accurately when the beam was degraded because of the enhanced errors in the forward direction. Comparison of these values in Table I confirms that all three methods are consistent. The only exceptions are for N^{14} and O^{16} bombardments of bismuth at high energies. The values obtained from symmetry considerations are lower than the calculated values here; this indicates that some reactions in which a compound nucleus is not formed may be contributing to the fission cross section at these energies.

Results of a similar nature were observed by Coffin with compound nuclei near these Z^2/A values.[31] On the other hand, Britt and Quinton have not reported any deviation from full momentum transfer for full-energy oxygen bombardments of bismuth.[20] As far as the c.m. angular distributions are concerned, the use of these two extreme values of $\bar{\eta}$ has little effect on the final interpretation of the data. This result will be discussed at greater length in Section IVB3.

Also listed in Table I are the values of the c.m. anisotropies, where

$$\text{anisotropy} = d\sigma(180 \text{ deg})/d\sigma(90 \text{ deg}) = d\sigma(0 \text{ deg})/d\sigma(90 \text{ deg}).$$

These values were calculated by extrapolating the lab angular distribution to 180 deg and applying the appropriate correction from Eqs. (2)

Table I. Values of eta and c.m. anisotropies for various systems and energies.

System	Energy (Mev)	Measurements	Degrader (mg/cm^2Be)	$\bar{\eta}_1$ [a]	$\bar{\eta}_2$ [b]	$\bar{\eta}_3$ [c]	c.m. anisotropy
$B^{11}+Au^{197}$	114.3	1	0	0.204	0.209	0.205	4.21±0.11
$C^{12}+Au^{197}$	124.6	3	0	0.220	0.228	0.221	4.17±0.12
	118.2	1	4.73	0.217	-	0.216	4.26±0.16
	112.1	1	9.45	0.211	-	0.210	4.05±0.16
	108.0	1	13.3(Al)	0.207	-	0.206	4.06±0.24
	81.0	2	28.4	0.182	-	0.178	3.71±0.15
	69.9	1	28.4+6.70(Al)	0.170	-	0.166	3.22±0.17
$N^{14}+Au^{197}$	145.4	2	0	0.251	0.251	0.255	3.96±0.14
	127.2	1	9.45	0.241	-	0.238	3.80±0.12
	107.0	1	18.9	0.221	-	0.219	3.48±0.10
	83.1	1	28.4	0.194	-	0.193	2.97±0.11
$O^{16}+Au^{197}$	166.1	1	0	0.286	0.29	0.288	4.37±0.24
	142.9	1	9.45	0.268	-	0.267	4.11±0.15
	116.8	1	18.9	0.240	-	0.242	3.64±0.14
	84.3	1	28.4	0.207	-	0.205	2.54±0.13
$B^{11}+Bi^{209}$	114.3	1	0	0.192	0.202	0.191	3.26±0.11
$C^{12}+Bi^{209}$	124.6	2	0	0.204	0.206	0.207	3.31±14
	112.1	1	9.45	0.197	-	0.196	3.19±0.14
	104.5	1	14.2	0.190	-	0.189	3.14±0.11
	97.4	1	18.9	0.184	-	0.183	3.11±0.17
	89.7	1	23.6	0.180	-	0.176	2.97±0.12
	81.0	1	28.4	0.171	-	0.167	2.74±0.10
$N^{14}+Bi^{209}$	145.4	2	0	0.232	0.237	0.239	3.31±0.08
	127.2	1	9.45	0.221	-	0.223	3.07±0.13
	107.0	1	18.9	0.208	-	0.205	2.68±0.13
	83.1	1	28.4	0.183	-	0.181	2.29±0.12
$O^{16}+Bi^{209}$	166.1	2	0	0.257	0.247	0.270	3.67±0.11
	142.9	1	9.45	0.241	-	0.250	3.52±0.12
	116.8	1	18.9	0.219	-	0.226	3.07±0.11
	84.3	2	28.4	0.193	-	0.192	1.89±0.11

[a] $\bar{\eta}_1$ based on symmetry about 90 deg

[b] $\bar{\eta}_2$ based on Eq. (4)

[c] $\bar{\eta}_3$ based on Eq. (5)

and (3) for the $\overline{\eta}$ value chosen for the final transformation. It was felt that this method would furnish the most reliable values of the anisotropy because the slope of the angular distribution near 180 deg is much flatter than in the same region in the c.m. system. The listed errors do not include possible errors in $\overline{\eta}$.

C. Center-of-Mass Angular Distributions

The transformed angular distributions for each heavy-ion--target system are shown in Figs. 15 through 22. Figure 23 summarizes the c.m. anisotropies as a function of bombarding energy. For the maximum energy bombardments, these values could be compared with the results of angular distributions measured by other workers. With B^{11}, C^{12}, and N^{14} incident upon gold, good agreement is found with recent counter experiments by Larsh and Sikkeland.[25] The present work agrees well with the experiments of Britt and Quinton[20] and Reynolds and Goldberg[21] for C^{12} on gold but are about 10% lower than the reports of Gordon et al.[19] Also, for O^{16} on gold there is agreement with Britt and Quinton, but a 10% deviation below Gordon's results. Britt and Quinton have examined C^{12} and O^{16} on bismuth, while Reynolds and Goldberg have measured N^{14} on bismuth. Both groups report values about 5% lower than this work.

From Figs. 15 through 23 we note that the c.m. angular distributions exhibit the following features:

1. Shape. At the maximum Hilac energies, the angular distributions can be described very well by the function $1/\sin\theta$ between 90 deg and 20 to 30 deg of the beam. Beyond this point, the data go through an inflection as they approach 0 deg. As one goes to lower energies, the data break away from the $1/\sin\theta$ function at angles nearer to 90 deg.
2. Target. For a given particle and bombarding energy, the anisotropy obtained with gold as the target nucleus is much greater than with bismuth. At lower bombarding energies the difference becomes smaller but is still distinct.

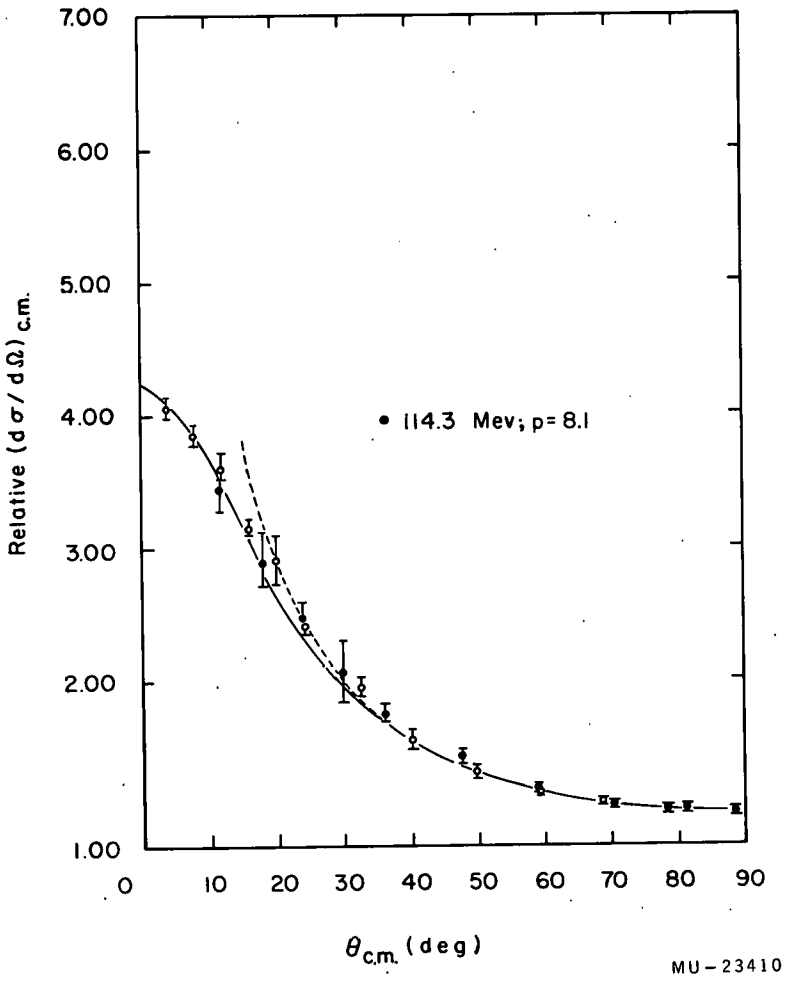

Fig. 15. Center-of-mass data from Au^{197} target bombarded with B^{11}. Solid curve is Halpern and Strutinski's theoretical fit; broken curve is the function $1/\sin\theta$. The differential cross section at 90 deg is unity. (Solid points refer to catcher angle θ; open points to angle $\pi-\theta$.)

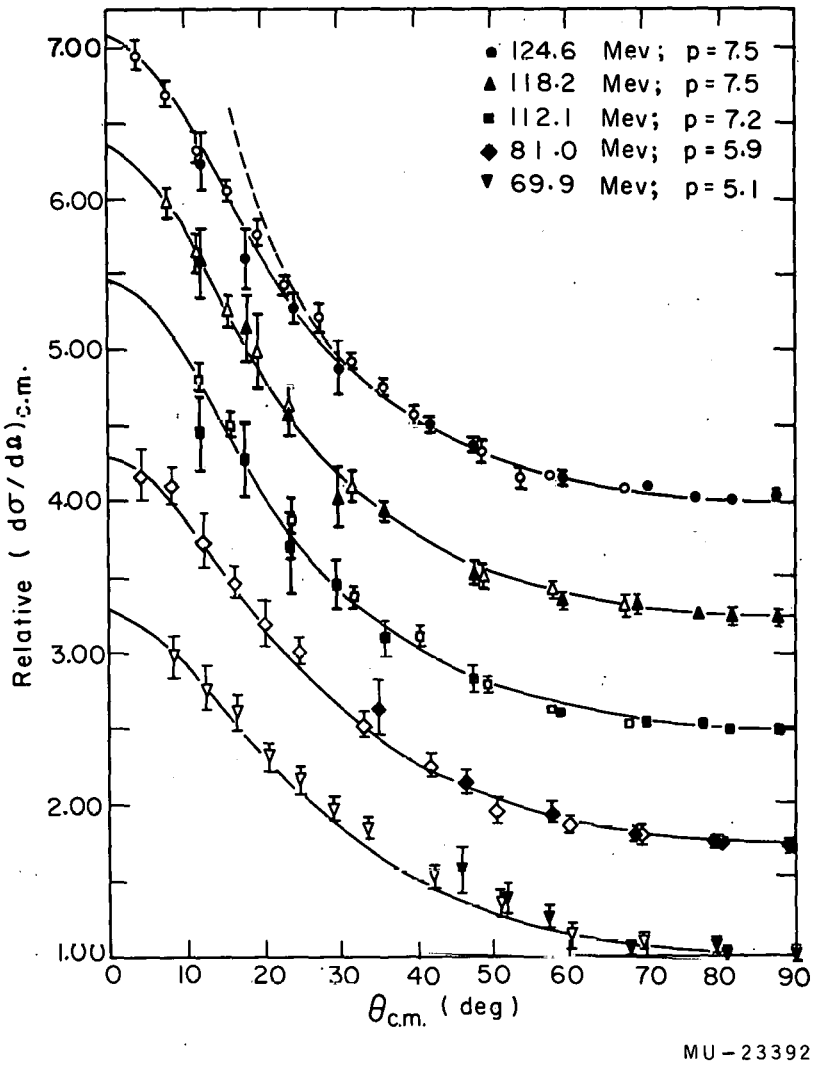

Fig. 16. Center-of-mass data from Au^{197} target bombarded with C^{12}. Solid curve is Halpern and Strutinski's theoretical fit; broken curve is the function $1/\sin\theta$. The differential cross section at 90 deg. is unity. (Solid points refer to catcher angle θ; open points to angle $\pi-\theta$.)

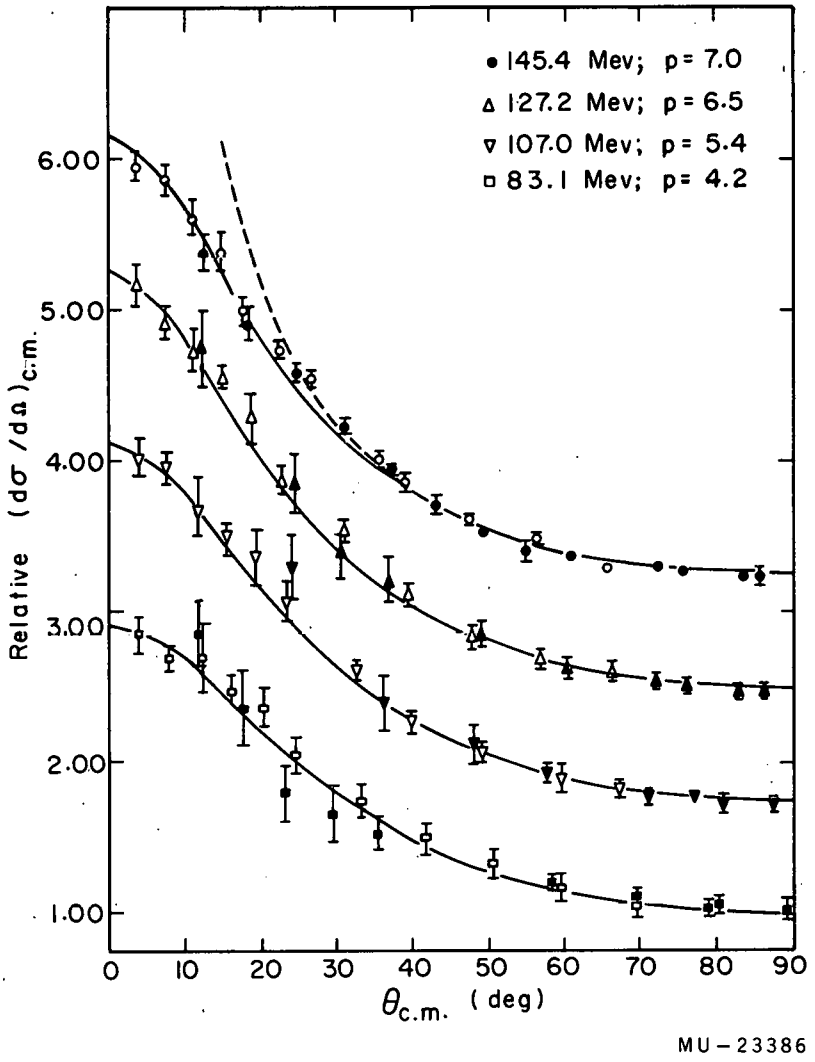

Fig. 17. Center-of-mass data from Au^{197} target bombarded with N^{14}. Solid curve is Halpern and Strutinski's theoretical fit; broken curve is the function $1/\sin\theta$. The differential cross section at 90 deg. is unity. (Solid points refer to catcher angle θ; open points to angle $\pi-\theta$.)

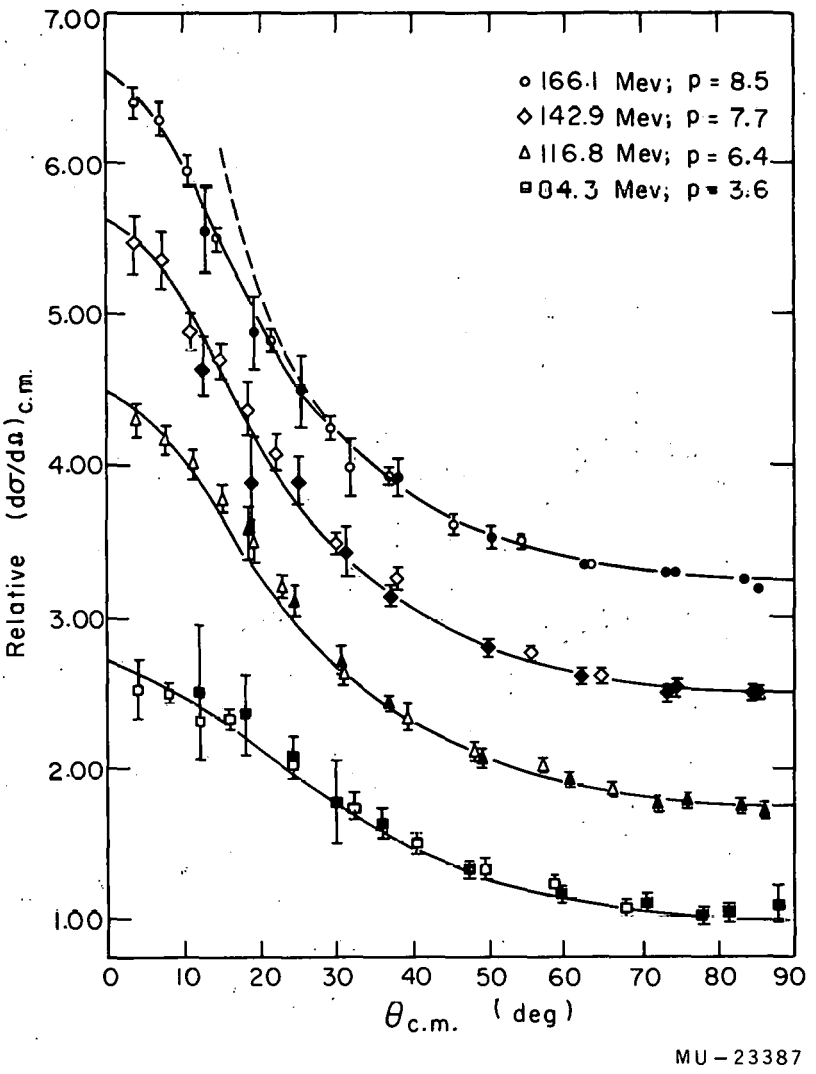

Fig. 18. Center-of-mass data from Au^{197} target bombarded with O^{16}. Solid curve is Halpern and Strutinski's theoretical fit; broken curve is the function $1/\sin\theta$. The differential cross section at 90 deg. is unity. (Solid points refer to catcher angle θ; open points to angle $\pi-\theta$.)

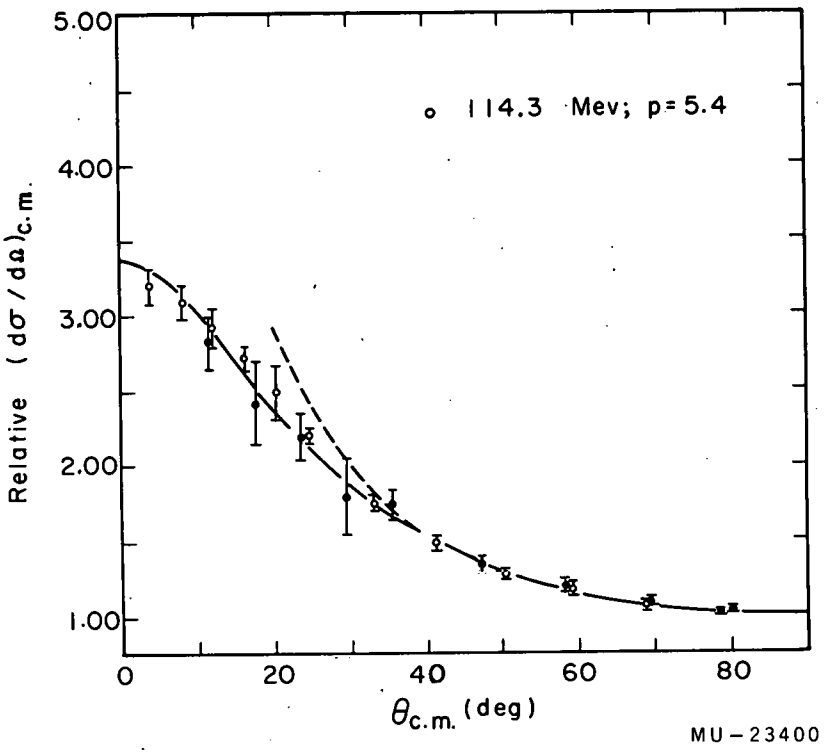

Fig. 19. Center-of-mass data from Bi^{209} target bombarded with B^{11}. Solid curve is Halpern and Strutinski's theoretical fit; broken curve is the function $1/\sin\theta$. The differential cross section at 90 deg. is unity. (Solid points refer to catcher angle θ; open points to angle $\pi-\theta$.)

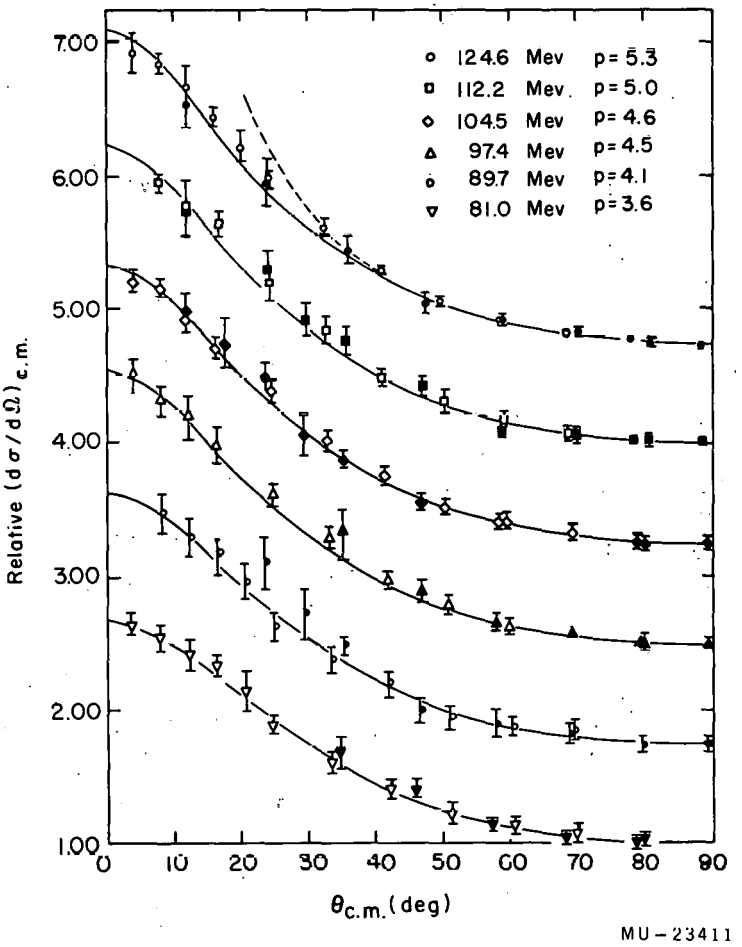

Fig. 20. Center-of-mass data from Bi^{209} target bombarded with C^{12}. Solid curve is Halpern and Strutinski's theoretical fit; broken curve is the function $1/\sin\theta$. The differential cross section at 90 deg. is unity. (Solid points refer to catcher angle θ; open points to angle $\pi-\theta$.)

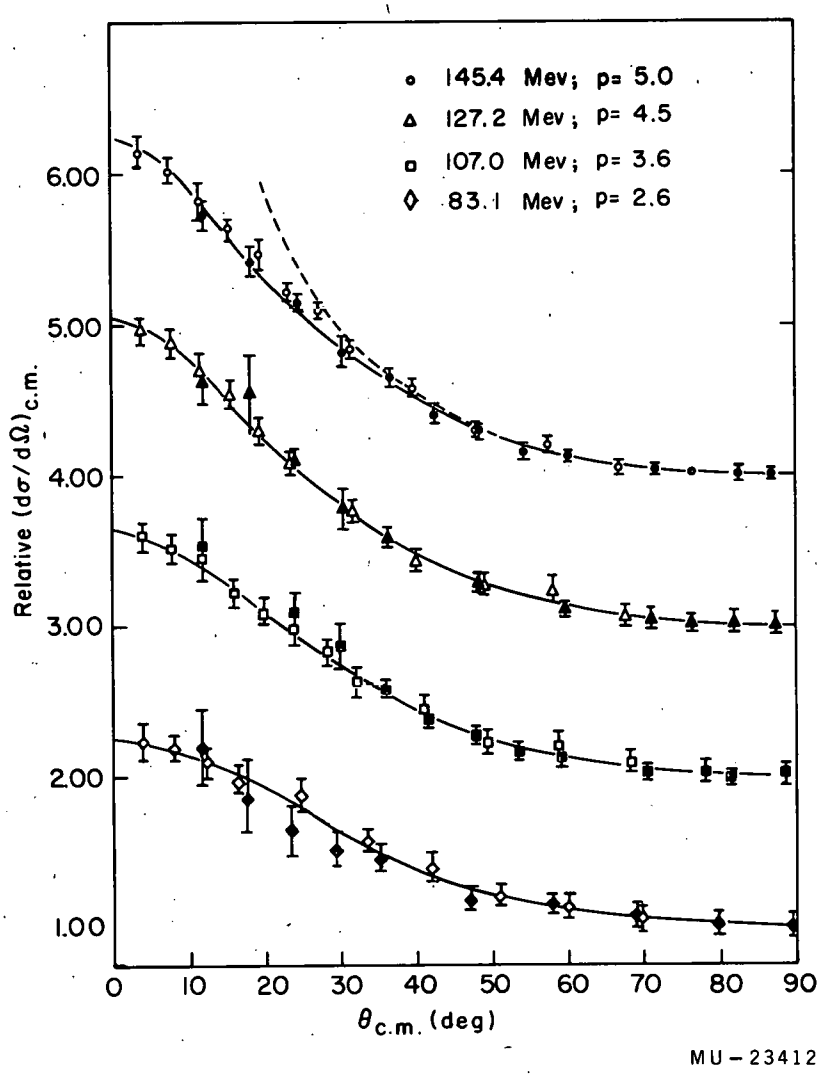

Fig. 21. Center-of-mass data from Bi^{209} target bombarded with N^{14}. Solid curve is Halpern and Strutinski's theoretical fit; broken curve is the function $1/\sin\theta$. The differential cross section at 90 deg. is unity. (Solid points refer to catcher angle θ; open points to angle $\pi-\theta$.)

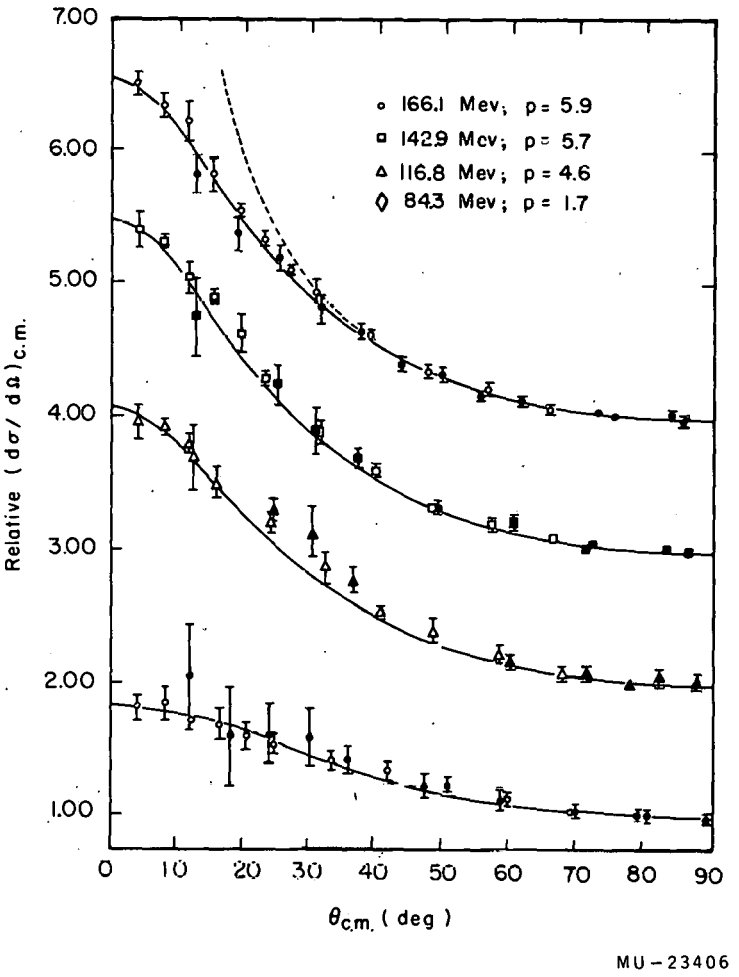

Fig. 22. Center-of-mass data from Bi^{209} target bombarded with O^{16}. Solid curve is Halpern and Strutinski's theoretical fit; broken curve is the function $1/\sin\theta$. The differential cross section at 90 deg is unity. (Solid points refer to catcher angle θ; open points to angle $\pi-\theta$.)

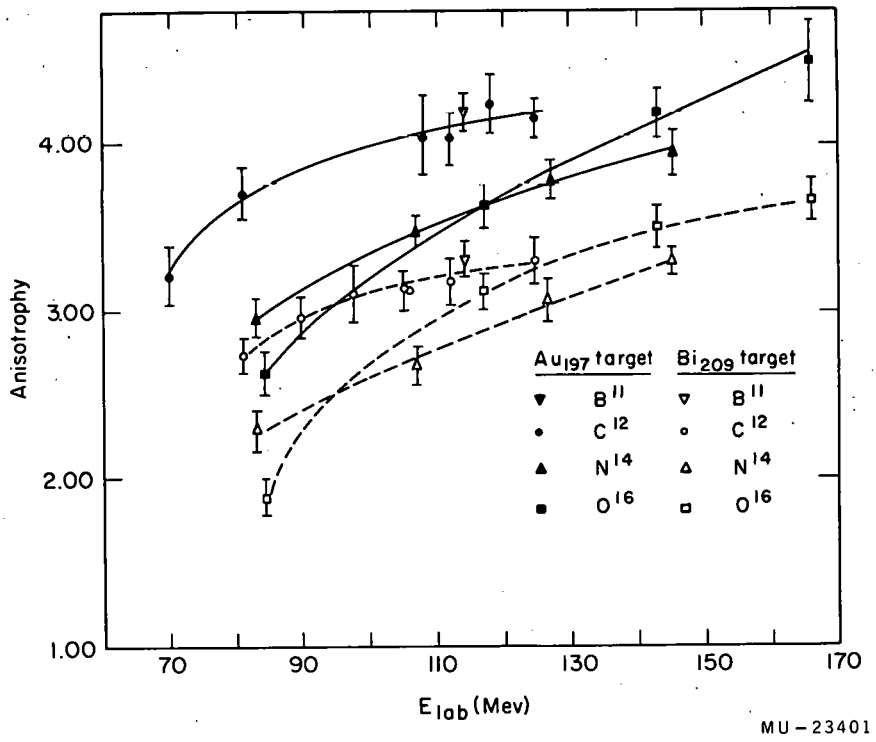

Fig. 23. Measured anisotropy as a function of bombarding energy (solid points: Au^{197} target, open points: Bi^{209} target; ▼ - B^{11}, ● - C^{12}, ▲ - N^{14}. ■ - O^{16}.)

3. Energy. Whenever a given target is bombarded with a specific heavy ion, the anisotropy decreases regularly with energy until within 20-30 Mev of the classical Coulomb barrier (assuming r_0 = 1.5 fermis). At this point there is a much more rapid decrease in anisotropy.

4. Heavy ion. Comparison of different heavy ions at high energy on the same target reveals that the greatest anisotropy is obtained with B^{11} and C^{12} followed in order by O^{16} and N^{14}. This is true for both gold and bismuth targets. At low energies the N^{14} and O^{16} curves cross one another.

IV. THE INTERPRETATION OF RESULTS

The interpretation of data from fission studies must take into account the complexity of this field of nuclear reactions. Particularly is this true with charged-particle-induced fission where, because of the Coulomb repulsion between the target and projectile, fairly high energies are necessary to initiate the reaction. This fact affords the compound nucleus a wide variety of de-excitation channels other than fission. Consequently, one must contend with reaction channels permitting the emission of gamma rays, neutrons, protons, and other charged particles in addition to the spectrum of fission channels leading to the observed distribution of masses (which, as pointed out in Section I, is still not satisfactorily explained).

Even if the nuclear potential were explicitly known, the level widths, Γ, of these de-excitation channels would be difficult to calculate because of the many nucleons involved. In lieu of this quantitative approach, it is convenient to examine these data in terms of some nuclear model. Although this cannot provide us with exact answers, considerable insight into the behavior of the fissioning nucleus can be gained.

A. Theory

The most elementary model for the description of fission-fragment angular distributions takes the form of an analogy to the classical flywheel. If the projectile is a sphere of charge Z_1e and energy E and the target is a sphere of charge Z_2e whose center is fixed in space, then the reaction can be represented as occurring in three steps:

(1) Collision (2) Absorption (3) Fission

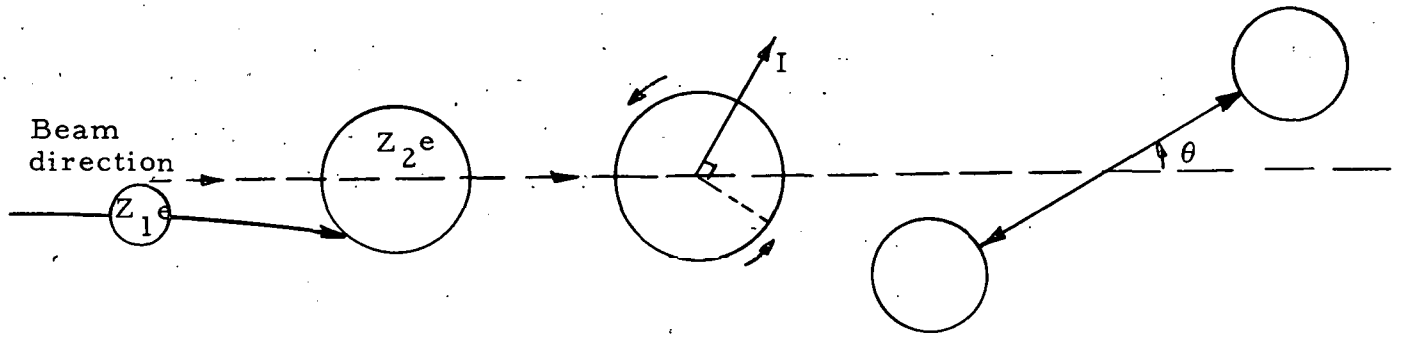

Unless the collision occurs at the center of the target area presented to the incoming particle, a compound system is generated that spins about an axis at right angles to the beam direction. The magnitude of the vector formed by the axis of spin describes the orbital angular momentum, ℓ, of the system.* The probability for the formation of a given angular-momentum state is $2\ell + 1$. This result is easily confirmed geometrically by consideration of the annular surface area of the target which will produce a given quantized state of angular momentum when struck by the projectile. The maximum value of ℓ depends primarily on the incident energy E and is given by

$$\ell_{max} = (R_1 + R_2) \left[2\mu \left(E - \frac{Z_1 Z_2 e^2}{R_1 + R_2} \right) \right]^{1/2} , \qquad (6)$$

where μ is the reduced mass of the system, and R_1 and R_2 are the respective radii. Classically, we have $\ell_{max} = (3/2)\,\bar{\ell}$, where $\bar{\ell}$ is the average value of ℓ. If the compound sphere breaks up, the two fragments must be emitted in a plane perpendicular to ℓ and at an angle of 180 deg with respect to one another. In this case ℓ is equal to the total angular momentum, I, because our spheres have no intrinsic spin. The probability of observing a fragment at any angle θ with respect to the beam should be equivalent; i.e.

$$d\sigma/d\theta = \text{constant.}$$

If we consider all possible collisions between the two spheres, the orientations of the angular-momentum vector are restricted to a plane through the center of the compound system and at right angles to the beam. Therefore, to obtain the total angular distribution (the

*In all these discussions, we have assumed $\hbar = 1$ and $c^2 = 1$ to simplify the formulas. Hence, all equations will have the dimension of energy (Mev) or length (c.m.). The relationship between these is 1 c.m.$^{-1}$ = 197.04×10^{-13} Mev and $e^2 = 1/137$.

number of fragments per unit solid angle), we must rotate the angular distribution found in a given plane by 180 deg.
This operation gives

$$W(\theta) \propto d\sigma/d\omega \propto d\sigma/\sin\theta d\theta \propto 1/\sin\theta.$$

This function should represent the maximum angular distribution that can be observed in any fission process involving compound-nucleus formation. Deviation from this idealized system--such as nonspherical nuclei or depolarization of the total angular momentum because of spins of the target or projectile--should cause the angular distribution to go below the value of $1/\sin\theta$. Such a model forms a useful visual basis for discussion of the results with respect to more detailed theories.

Bohr has suggested the framework for a comprehensive theory of fission angular distributions from considerations of the nuclear excitation energy as well as the spin of the compound nucleus.[16] At energies near the fission threshold, E_f, most of the available nuclear-excitation energy, E^*, is absorbed in nuclear deformation. This creates a "cold" nucleus at the fission saddle point; thus the available fission channels should resemble the low-lying energy states of stably deformed nuclei. Bohr assumes that the nucleus retains axial symmetry throughout the fission process and that the fragments are emitted along this axis. The following diagram describes the quantum states of the fissioning nucleus, where K is the projection of the total angular momentum I on the nuclear-symmetry axis, and M is the projection of I on the beam direction. According to this picture, the angular distribution depends on the orientation of the nuclear-symmetry axis as well as that of the spin axis. For a compound nucleus with quantum numbers I, K, and M, the angular distribution is given by the square of the symmetric-top wave function $|D^I_{KM}(\theta)|^2$. In fission induced by medium-energy particles, the angular-momentum transfer of the reaction is large so that $\ell \tilde{=} I \gg M$.

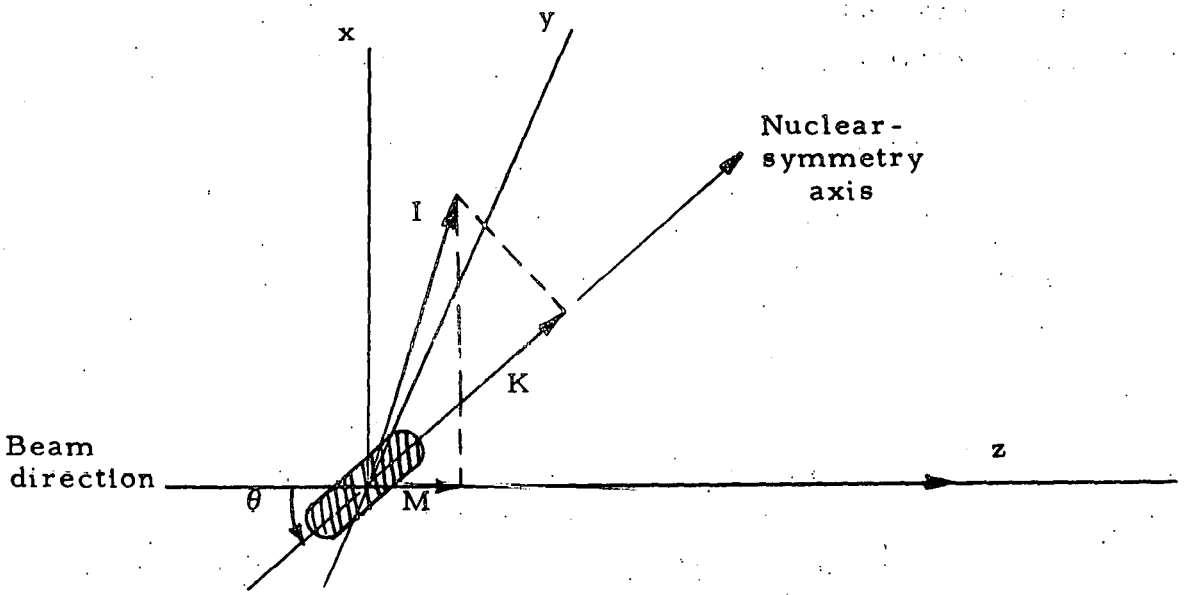

By setting $M = 0$ and averaging over the distributions of K and I, F(K) and G(I), one obtains

$$W(\theta) = N \int_0^{I_{max}} dI \int_{K \leq I \sin\theta}^{K_{max}} dK\, F(K)\, G(I)/(\sin^2\theta - K^2/I^2)^{1/2}, \qquad (7)$$

where N is a normalization factor.

Halpern and Strutinski and, independently, Griffin have extended Bohr's theory to fission reactions induced by medium-energy particles.[17, 18] Because the angular momentum associated with heavy-ion reactions is usually quite large, the assumptions that M=0 and $I=\ell$ should be quite good for these comparisons. As mentioned in Section I, the enhanced probability for compound-nucleus formation with heavy ions provides states of high excitation energy and angular momentum. Because K is related to the deformation of the nucleus, it should describe the channels available for fission and hence, the excitation energy. The function G(I) should be reasonably approximated by the classical distribution of spin states:

$$G(I) \propto I; \quad I \leq I_{max}$$

$$G(I) = 0; \quad I > I_{max}.$$

This classical approach is used in both treatments.

The primary difference in the two theories stems from the function assumed for F(K). Halpern and Strutinski propose a distribution of fission channels based on statistical theory. If the level density of the internal states is high, then they assume

$$F(K) \propto \exp(-K^2/2K_0^2),$$

where K_0^2 is the mean value of K^2. Substituting this function into the Bohr formula of Eq. (7), they obtain

$$W(\theta) = N' \int_0^{I_{max}} dI \; I\, G(I) \exp(-I^2 \sin^2\theta/4K_0^2)\, J_0(iI^2 \sin^2\theta/4K_0^2), \qquad (8)$$

where J_0 is the zero-order Bessel function. The integration over I gives the angular distribution in terms of the anisotropy parameter,

$$p = I_{max}^2/4K_0^2$$

Halpern and Strutinski extend their discussion to an analysis of K_0 as a function of excitation energy. According to statistical theory, at high excitation energies, we can write

$$K_0^2 \propto (E^* - E_f)^{1/2}.$$

However, at low energies the experimental results from neutron fission of Th^{232} favor a linear dependence of K_0^2 on $(E^* - E_f)$. In the intermediate region, the dependence $K_0^2(E^* - E_f)$ was determined empirically from studies of alpha-particle induced fission with Np^{237}.

Griffin derives F(K) from a fit to the discrete distribution of harmonic-oscillator shells, using the continuous approximation:[18]

$$F(K) = K - K_{max} \quad ; \quad K \leq K_{max}$$

$$F(K) = 0 \quad ; \quad K > K_{max}.$$

With this distribution, he gets

$$W(\theta)/W(90\ \text{deg}) = (1 - 3x/4)^{-1} \tag{9}$$

for $x < 2$, and

$$\frac{W(\theta)}{W(90\,\text{deg})} = \frac{\pi}{6}\left[\frac{\arcsin(2/x)}{3} - \frac{x - (x^2 - 4)^{1/2}}{8} + \frac{(x^2 - 4)^{1/2}}{12x^2} + \frac{\ln(1/2)}{3x^3}\left\{x + (x^2 - 4)^{1/2}\right\}\right]^{-1}, \tag{10}$$

for $x > 2$, where we have $x = r\cos\theta$, and r is the ratio of the average value of I to the average value of K, $\bar{I}/\bar{K}$. Thus, r is analogous to the p parameter of Halpern and Strutinski. Griffin's prediction for the function $\bar{K}(E^* - E_f)$ at low energies was obtained empirically from neutron fission of Pu^{239} and, as in the previous work, he finds a linear function fits best. Griffin also predicts that, at high energies, $\bar{K}$ should follow a square-root dependence on $(E^* - E_f)$ but does not indicate the point at which this change should occur.

Qualitatively, these two treatments forecast the same relationship between the anisotropy (p or r) and the primary factors that control the fission process. Both predict that the observed anisotropy will increase with greater orbital-angular-momentum transfer in the reaction. As more fission channels become available, i.e. as the excitation energy increases, the anisotropy should decrease. Finally, because the height of the fission barrier governs the availability of fission channels, the anisotropy should decrease as the barrier becomes lower. Thus, one should observe lower angular distributions as Z^2/A of the compound nucleus increases because increasing this parameter is known to decrease the fission barrier. In Section IV C 1 specific differences in the predicted angular distributions will be compared in terms of the experimental data.

B. Factors which Influence the Anisotropy

Before attempting an explicit application of the theory, let us first examine the qualitative correspondence between the data and the model of fission that has been discussed in the previous section. These considerations should act as a guide in testing the fundamental applicability of the theory to heavy-ion results. It is of further interest to compare the observations from this work with the conclusions drawn at lower energies (Section I.).

Several properties of the fissioning compound nucleus contribute to the angular distribution, some calculable and others not. The angular momentum is of primary significance. The values for all $\overline{\ell}$ discussed in this work are based on the calculations of Thomas, assuming a square-well nuclear potential with $r_0 = 1.5$ fermis.[38] A knowledge of the excitation energy is also essential. For the original compound nucleus, this quantity has been calculated from the formula

$$E^* = E_{c.m.} - (M_{CN} - M_p - M_t) \qquad (11)$$

where $E_{c.m.}$ is the center-of-mass kinetic energy of the projectile and M_{CN}, M_p, and M_t are the masses of the compound nucleus, projectile, and target, respectively. Measured masses were used for the projectile, while the mass tables of Cameron defined the masses of the heavier nuclei.[39]

Many other forms of de-excitation compete with fission in these reactions, so that the excitation energy at the instant of each fission event is of greater importance than the initial excitation energy. At this point we encounter the primary difficulty in the analysis of these results. For nuclei with Z less than 90, there is a lack of experimental information concerning Γ_j/Γ_f, particularly for the neutron-deficient isotopes of a given element. Here Γ_j represents the level width for de-excitation from reaction channels other than fission, and Γ_f is the level width for fission. This point is discussed at greater length in

Section IVC. On this account, it should be stressed that the ensuing discussion is restricted to the average fission process.

In Figs. 24 through 26, the experimental anisotropies are plotted as a function of the difference between the bombarding and Coulomb-barrier energies, the average angular-momentum transfer, and the initial excitation energy. The lines connecting the points have no significance other than to correlate the data.

1. Target

Examination of the anisotropies obtained with the same heavy ion incident upon both targets reveals that the gold target produces a much greater forward-backward peaking of the fission fragments than does bismuth. In terms of the model we have assumed, this fact is explained in a straightforward manner. The compound nucleus formed from gold has a much lower Z^2/A value. This implies that the fission barrier is higher and, as a result, fewer fission channels are open; i.e., the average value of K is reduced. On the other hand, the average angular-momentum transfer at the same bombarding energy is nearly the same for these two targets. Therefore, the average anisotropy parameter ($I_{max}^2/4K_0^2$ or $\overline{I}/\overline{K}$) should be lower with bismuth.

One can extend the examination of this result to infer some knowledge of Γ_j/Γ_f for these elements. Taking the specific example of 124.6-Mev C^{12} bombardments with both targets, we produce two compound nuclei with nearly the same orbital angular momentum: At^{209} ($E^* = 101$ Mev; $Z_2/A = 34.6$) and Ac^{221} ($E^* = 86$ Mev; $Z^2/A = 35.5$). By comparison of the trends from known and estimated values of the fission barrier heights[12, 13, 40] and also from the formulae of Pik-Pichak and Hiskes, it can be reasonably assumed that the fission barriers for these two nuclei should not differ by more than 5 to 10 Mev. This means that initially $(E^* - E_f)$ and the average value of K must be larger for At^{209} than for Ac^{221}. The experimental anisotropies indicate that if the angular momentum is the same, there must be fewer fission channels available to At^{209} than to Ac^{221}. Consequently, the astatine nucleus

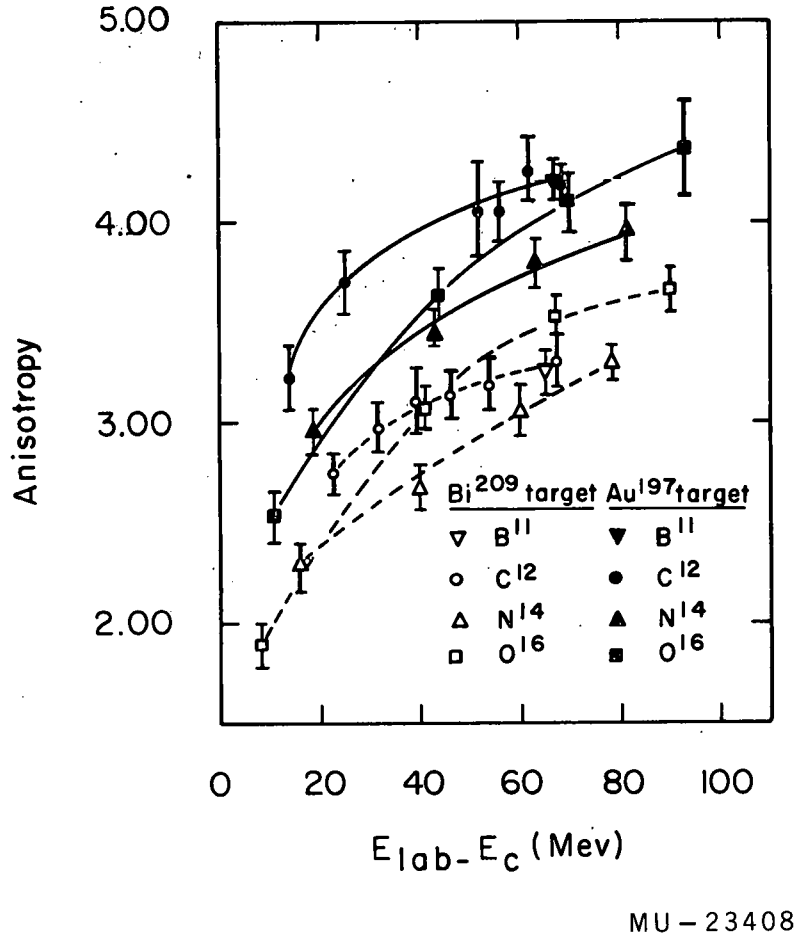

Fig. 24. Measured anisotropy as a function of the difference between the bombarding energy and the classical Coulomb barrier.

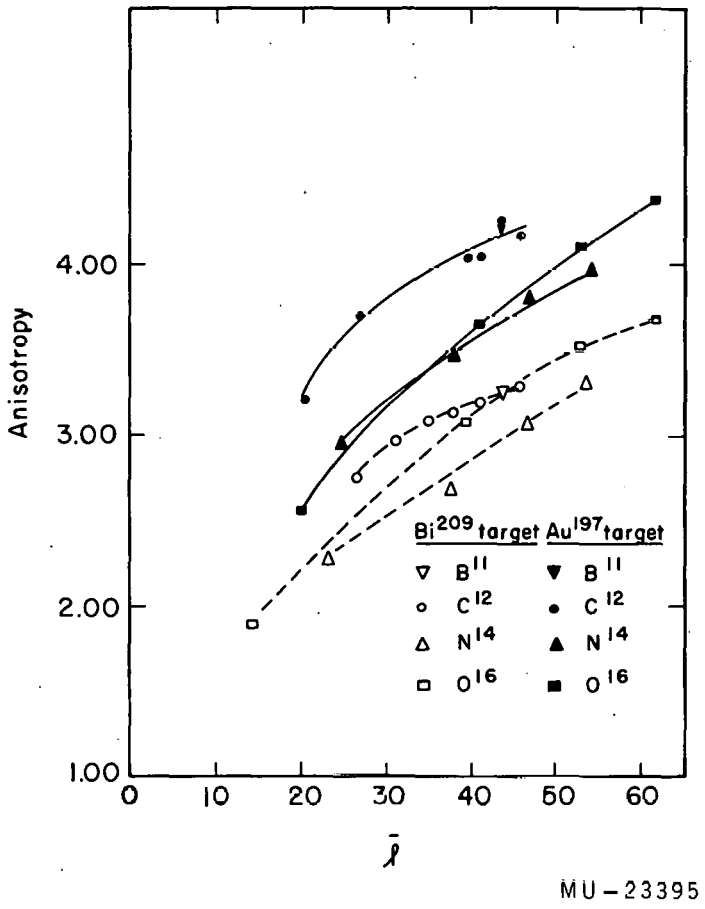

Fig. 25. Measured anisotropy as a function of the average angular-momentum transfer.

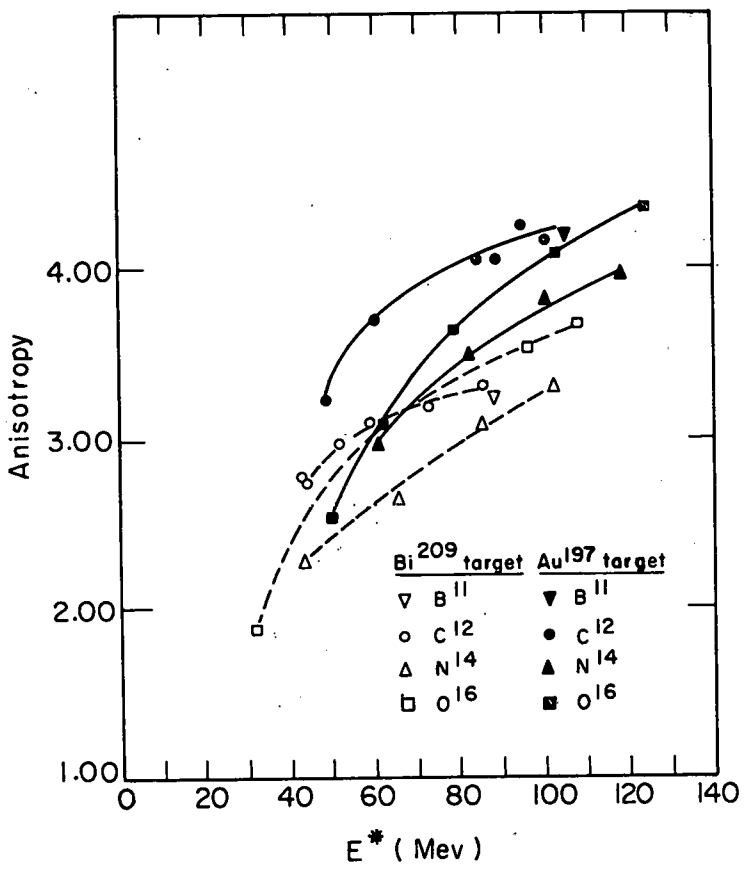

Fig. 26. Measured anisotropy as a function of the excitation energy.

must release considerable energy before the average fission event occurs, presumably in the form of particle evaporation. Latimer has measured the cross sections for the production of astatine spallation products from 120-Mev carbon on gold, and finds a value of about 100 mb for At^{201}.[41] Thus a large number of the compound nuclei are successfully competing with fission through the evaporation of eight neutrons, From these arguments, one is lead to suggest that a substantially larger number of light particles are discharged from the compound-nucleus At^{209} before fission than from Ac^{221}. This is in good agreement with the conclusion of Fairhall et al. that Γ_n/Γ_f exhibits a marked increase with decreasing Z of the compound nucleus.

There is an alternative explanation of this dependence of the anisotropy on target that should be noted. The spin of Au^{197} is 3/2, while that of Bi^{209} is 9/2. It is possible that the larger spin of the bismuth nucleus couples with the orbital angular momentum of the reaction in such a way as to depolarize the total angular momentum; i.e., the assumption that M equals zero is incorrect so that $\overline{I}$ is less than $\overline{\ell}$. Although this would diminish the forward-backward peaking for reactions with bismuth targets, it is doubtful that such a large effect would result. Furthermore, several experiments with neutrons and charged particles at lower energies have demonstrated no dependence of the angular distribution on target spin.[11,42,43]

2. Bombarding Energy

The dependence of the anisotropy on heavy-ion bombarding energy is generally similar to that reported with lighter particles, except much larger in magnitude. Figure 24 reveals that just above the Coulomb barrier the anisotropy increases rapidly, but thereafter increases only gradually with energy. The calculated increase in orbital angular momentum as a function of bombarding energy exhibits analogous characteristics. A comparison of Figs. 24 and 25 reflects this correspondence, one that would be expected from Eq. (6). One additional correlation with the calculations of Thomas can be inferred

from the substantial anisotropy of 1.9 obtained from oxygen on bismuth only a few Mev above the classical Coulomb barrier. This observation is consistent with Thomas' prediction that heavy ions at low energy can transfer more angular momentum than classically permitted. That the increase in anisotropy with bombarding energy is at least partially an angular-momentum effect has been shown by Coffin and Halpern.[11] They prepared identical compound nuclei of the same excitation energy but quite different angular momenta and found that the larger angular momentum effected a larger anisotropy.

Although there exists a general correspondence between the rate of increase of angular momentum and the anisotropy, the absolute magnitude of this effect is far from consistent with an analysis of the data in terms of spherical harmonics of order ℓ. This has been discussed by Wigner.[44] For a classical collision between two spheres, in which the reaction products have no intrinsic angular momentum, the total angular distribution per unit solid angle is $(2\ell+1)^2 \left|P_\ell(\cos\theta)\right|^2$, where $P_\ell(\cos\theta)$ is the Legendre polynomial of order ℓ. From this point of view, Wigner estimates that for carbon on gold with $\ell_{max} = 55$ the anisotropy should be about 100, whereas a value of 4 is observed.

Of course, the above considerations are highly idealized, but they do imply that rather strong forces oppose the influence of the angular momentum on the resultant angular distributions from fission. Transferring this evaluation to the theoretical framework presented in Section IV.A., we remember that the anisotropy should vary inversely with the average value of K. From the dependence of K on excitation energy, then, it is logical to postulate that the anisotropy should decrease with increasing excitation energy in systems possessing identical total angular momentum. Indirect evidence to support this statement can be found among several radiochemical angular-distribution studies at low energy.[45-47] These experiments report the anisotropy for symmetric fission fragments to be much lower than for asymmetric fragments. If symmetric fission occurs at high energy and asymmetric division is a low-energy process as suggested by Farihall,[24] then this conclusion is justified.

One can picture this competition between angular momentum and excitation energy as follows. Consider two rotating liquid drops of the same angular momenta, one of which is rapidly undergoing random surface distortions due to internal excitation energy, while the other is cold and maintains a constant shape. The vectors which describe the modes of motion of the distorted drop may have orientations in three dimensions; those of the uniform drop are restricted to a plane. Thus, if separation occurs, the distorted drop should divide with less concern for its axis of rotation, and therefore be less anisotropic when the process is averaged over all space (cf. the flywheel model in Section IV A.). Nonetheless, no matter how violently the former drop deforms, as long as it has a finite lifetime, it must always show some preference to its axis of rotation when it divides. For this reason, one qualitatively expects that the angular momentum should be somewhat more important than the excitation energy in regulating the anisotropy.

In terms of this analogy, the experimental results are readily explained. At energies well above the Coulomb barrier, the heavy ion always deposits large amounts of both angular momentum and excitation energy. Increasing the bombarding energy tends to increase simultaneously the already large rotational forces and surface deformations. It is reasonable to hypothesize that the ratio of these two factors will remain relatively constant. The slightly greater importance of the angular momentum should cause the anisotropy to increase slowly with energy. In contrast, near the Coulomb barrier the angular momentum decreases rapidly, while the excitation energy remains a linear function of the bombarding energy. The result is a sharp decrease in the anisotropy near the Coulomb barrier.

The preceding discussion demonstrates that the experimental observations can be interpreted in terms of the theory, at least from an elementary standpoint. Still, several other effects could produce the same outcome, as has been pointed out by Wigner.[44] It is entirely possible that the orbital angular momentum of the interaction is not as large as assumed, and not necessarily oriented perpendicular to the

beam direction. This will be discussed further in the next section. Another possibility is that particle evaporation may carry off sizeable amounts of angular momentum before fission takes place. From consideration of transmission probabilities for ℓ-wave neutrons, Halpern and Strutinski calculate that, to the first order, the angular momentum of the compound nucleus should be unchanged.[17] A more detailed approach has been taken by Thomas, who estimates, on the basis of the level-density predictions of Ericson and Strutinski,[48] that one neutron evaporated from At^{209} at 95-Mev excitation energy and $\ell_{max} = 66.5$ decreases ℓ_{max} by about one unit.[49]

Finally, if the fission fragments are formed in states of high intrinsic angular momentum, the observed angular distribution should be lower than would be predicted by a harmonic analysis. Studies of isomer ratios from fission products have shown that the population of high spin states increases with bombarding energy, i.e. with greater angular-momentum transfer in the reaction.[50] Thus, it is quite likely that part of the observed lowering of the anisotropy can be attributed to such an effect.

One additional source of error in the estimates of the spin of the compound nucleus works in the opposite direction. If several neutrons are emitted before fission, the remaining compound nuclei possess low excitation energies and a distribution of spin states. If the nuclei with high total angular momentum are more fissionable and the low spin states prefer to de-excite by neutron evaporation, the average value of I for the fissioning nuclei would be higher.

3. Projectile

One of the original aims of this research was to form a series of related compound nuclei in hopes of gaining some insight into the nature of the fission process as a function of Z and Z^2/A. From inspection of Figs. 23 through 28, it appears that although such relationships may exist, they are not described in simple terms.

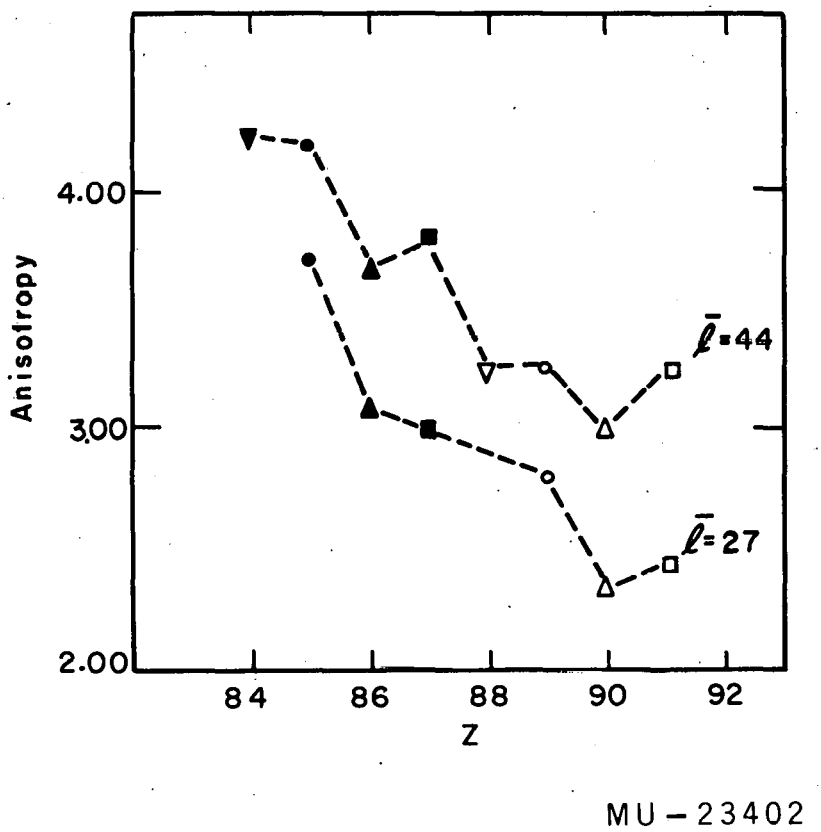

Fig. 27. Measured anisotropy as a function of Z. The symbols used for the points in Fig. 26 apply here.

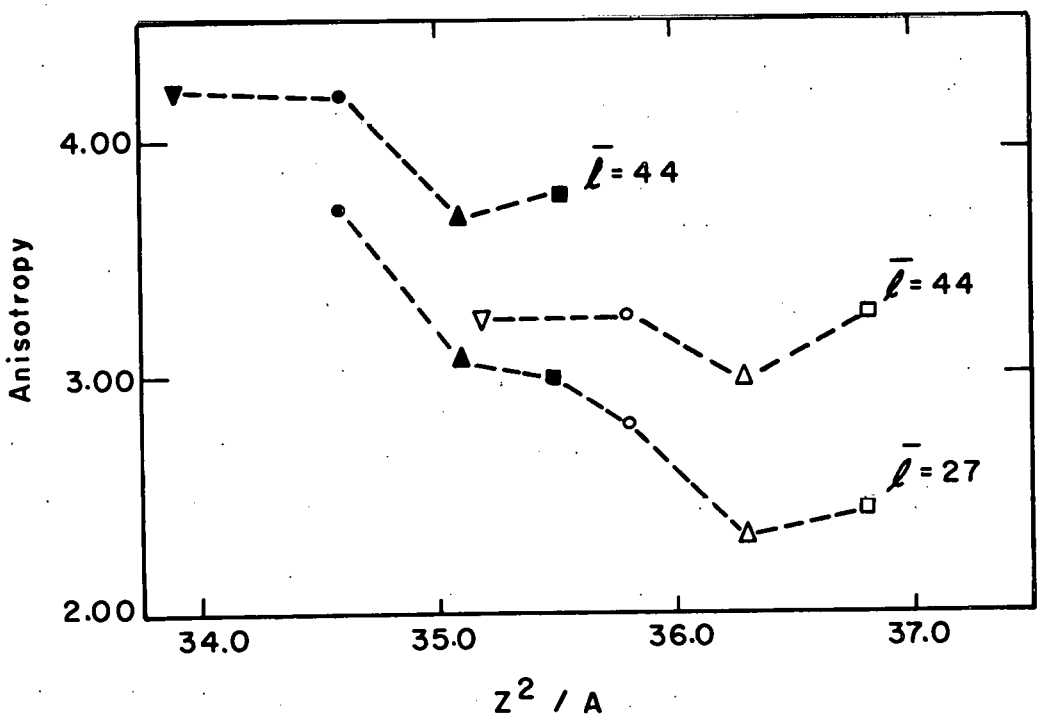

Fig. 28. Measured anisotropy as a function of Z^2/A. The symbols used for the points in Fig. 26 apply here.

In common with the results from low-energy fission, we have already noted that these angular distributions are peaked along the beam direction and gradually become more anisotropic as the bombarding energy increases. Furthermore, consideration of the same projectile on different targets confirms that the anisotropy shows a pronounced decrease with increasing Z^2/A. In contrast with the low-energy work, an increase in the anisotropy with the size of the projectile is not observed. Such behavior should not necessarily be expected with heavy ions. The low-energy conclusions were derived from projectiles whose masses differed by factors of two to four, whereas with heavy ions the increment of mass change is only a small percentage of the total mass. Therefore, differences in the fissionability and level widths for other de-excitation processes assume greater significance for heavy ions.

Because the forward-backward peaking is known to decrease with increasing Z^2/A of the compound nucleus, it is reasonable that, for the same target, increasing anisotropy could be observed with decreasing rather than increasing projectile mass. However, it was expected that, for systems of nearly the same angular momentum and excitation energy, the anisotropy should manifest some sort of regular behavior with Z or Z^2/A. This is not confirmed experimentally as is seen in Figs. 27 and 28. Although corrections for small effects due to initial excitation energy would improve the correlation, it seems unlikely that the results can be described by any monotonic function of Z^2/A as has been done at lower energy.[11] It is interesting to note, however, that in going from $\bar{\ell} = 44$ to $\bar{\ell} = 27$, the anisotropies appear to become more closely related to Z and Z^2/A. Thus, the discrepancy seems to be connected with the bombarding energy.

Figure 24. indicates rather parallel behavior for each ion-target pair. However, Figs. 24 through 28 reveal that, in general, N^{14} produced anisotropies are lower than those from C^{12} and O^{16}. The two points for B^{11} are difficult to characterize, but may be slightly low.

To attempt an explanation of this anomaly, let us examine in which respects the several target-projectile systems differ. The bombarding particles fall into two classes: (1) carbon and oxygen with all nucleons paired in closed single-particle shells or subshells, and (2) boron and nitrogen having unpaired nucleons that result in nuclear spins of 3/2 and 1, respectively. The second set is considered more loosely bound than the first. Both targets are odd-even nuclei, so that a series of compound nuclei from Z = 84 to 91 is obtained. Thus, one forms compound nuclei of odd Z with carbon and oxygen, and of even Z with boron and nitrogen.

It was first suspected that the lower anisotropies observed in the even-Z compound systems were the result of level-density effects from several stages of neutron evaporation. In fission-spallation competition studies at lower energy, Vandenbosch et al. have argued that de-excitation by neutron emission to odd-A states should be favored over decay to even-even states because of the higher density of available levels in the former case.[51] Consistent with this reasoning, one could propose that because of the possibility of even-even nuclei appearing several times in a many-neutron decay chain from even-Z compound nuclei, the average value of Γ_f/Γ_n might be larger for even-Z than odd-Z nuclei. This consequence would encourage fission events at higher energy, and thereby lower the anisotropy for even-Z compound nuclei.

This viewpoint is not very consistent with the high initial excitation energies in these systems and, in addition, no evidence has been reported of such effects in angular distributions at lower energy. Furthermore, emulsion studies by Reynolds and Goldberg contradict this argument.[21] Their results from maximum Hilac energy bombardment of Pb^{208} give $d\sigma(175\ deg)/d\sigma(90\ deg)$ ratios of 3.2 for C^{12}, 2.7 for N^{14}, and 3.0 for O^{16}. Although the magnitude of some of these values is somewhat at variance with our work on the neighboring target nucleus of bismuth, it is noted that N^{14} gives the lowest anisotropy. In this case, nitrogen forms an odd-Z compound nucleus, and in this light, the preceding arguments appear improbable. The conclusion one seems

forced to accept from these considerations is that the anomaly originates in the collision process and not in the de-excitation events. This is not a very satisfactory tenet from the standpoint of a more exhaustive interpretation of the data, because it implies a breakdown of our assumptions about the classical nature of nuclear reactions induced by heavy ions.

In searching for an alternative explanation, the most promising area appears to be the nuclear-surface reaction. These reactions, which are estimated to have a total cross section of several hundred millibarns, are postulated to proceed through a "grazing contact" mechanism that involves penetration of the Coulomb barrier but not compound nucleus formation.[52] These interactions lead to inelastic scattering, nucleon transfer, or breakup of the projectile. It is conceivable that the unpaired nucleons and lower binding energy of the boron and nitrogen nuclei might make them more susceptible to such reactions. According to the arguments of the previous section, these surface reactions may take place at the expense of compound-nucleus formation. Thus, many of the high angular-momentum states will be lost, and $\overline{\ell}$ will be lower than calculated.

From the currently available data, it is difficult to draw any correlations between the surface reactions and fission angular-distribution results. Wolfgang and Kauffman have investigated nucleon transfer reactions with C^{12}, N^{14}, O^{16}, and F^{19}, but on lighter targets than studied here.[52] Their thick-target data from silver bombardments show nitrogen and fluorine to give anomalously high yields wherever comparisons can be made. However, thin target yields from rhodium do not necessarily support the same conclusion. The excitation functions from their work show that the amount of nucleon transfer decreases rapidly at lower energies--a result consistent with the decrease in the anisotropy anomaly at lower energy (Fig. 27). Britt and Quinton have studied the alpha-particle spectrum from heavy-ion bombardments of gold with C^{12}, N^{14}, and O^{16}.[53] Their estimates of the evaporation cross

sections (100 to 200 mb) for alpha particles show no unusual behavior with different ions. They report direct-interaction cross sections from Au^{197} of 0.83 barns for 126-Mev C^{12}, 0.56 barns for 147-Mev N^{14}, and 0.54 barns for 165-Mev O^{16}. All of these cross sections decrease rapidly with bombarding energy. The authors attribute these results to a breakup of the projectile at the nuclear surface. From our point of view, the amount of reaction at the nuclear surface seems to be lower for N^{14} than for C^{12} and O^{16}. However, if a sizeable fraction of the alpha-deficient residues are absorbed by the target, the subsequent compound nuclei would have lower Z^2/A values. Our previous arguments imply that any fission reactions originating in these states should be more anisotropic. From this line of reasoning, the bombardments with oxygen and carbon might be expected to be more anisotropic.

If reactions involving breakup of the incoming particles contributed substantially to the fission cross section, however, it should be reflected in the c.m. transformation parameters. Table I shows that, in general, there is excellent agreement with full momentum transfer of the projectile to the compound nucleus. The notable exceptions to this are N^{14} and O^{16} at the maximum Hilac energies incident upon bismuth. The deviations range up to 5% for full-energy oxygen. In these cases it is possible that breakup reactions are affecting the data. This has also been suggested by Gordon et al. to explain the results of uranium fission induced by C^{12}.[54]

In summary, the anomalous behavior of the fission-product angular distribution from nitrogen, and possibly boron, with respect to carbon and oxygen is only tenuously explained. Further angular-distribution studies with boron, fluorine, and neon as projectile ions should help resolve this discrepancy. Examination of surface-reaction phenomena on a single heavy target as a function of heavy-ion mass should also provide an interesting comparison with these data.

C. Numerical Analysis of the Angular Distribution Data

To perform an exact analysis of the data in terms of the theories of Halpern and Strutinski and of Griffin, one must know all the level widths, Γ_i, involved in the de-excitation processes. The angular distribution of the fission fragments from the initial compound nucleus can be calculated from the excitation energy (which fixes K) and the total angular momentum. This result is then weighted by the probability for "first-chance" fission, $\Gamma_{f1}/\Gamma_{f\ total}$, to obtain this state's contribution to the total angular distribution. The remainder of the initial nuclei will de-excite through other channels to daughter compound nuclei, the relative amounts of each being determined by $\Gamma_{1n}/\Gamma_{total}$, $\Gamma_{1p}/\Gamma_{total}$, etc. If we assume that the average value of I is unchanged, the excitation energy of each of these products can be calculated, and a new series of angular distributions is provided. These are weighted accordingly for "second-chance" fission, and the procedure carried on to the next stage until all fission events are accounted for. The final angular distribution is

$$W(\theta) = \sum_k \frac{\Gamma_{fk}}{\Gamma_{f\ total}} \cdot w(\theta)_k \ , \qquad (12)$$

where k represents a specific compound nucleus at a fixed excitation energy and $w(\theta)_k$ is the angular distribution from that state. This result, then should be compared with the final data to test the validity of our assumptions. Pik-Pichak has derived the proper theoretical form for consideration of the effects of neutron evaporation on the angular distribution.[55]

It has been pointed out already that the lack of experimental information concerning the level widths for these isotopes precludes the possibility of a rigorous comparison of theory and experiment. For nuclei near the line of stability with $Z < 90$, Fairhall et al. have reported that (a) Γ_f/Γ_{total} depends strongly on Z, but only weakly on A,

and (b) Γ_f/Γ_{total} at first increases markedly with excitation energy, and then levels off above 35 Mev.[24] The behavior of Γ_f/Γ_{total} above 35 Mev is difficult to predict. The calculations of Ericson and Strutinski indicate that the density of internal states is high at high excitation energies, so that the level width for neutron evaporation should be enhanced.[48] Opposing this factor, the lowering of the fission barrier for states of high angular momentum, should add to the probability for fission, discussed earlier. In Appendix B, these several considerations are used in an attempt to treat a specific angular distribution according to the manner prescribed above.

As an alternative to knowledge of the individual level widths, we can adopt a less sophisticated approach and ask "What can we learn about the average fission process from the experimental data?" The theoretical anisotropy parameter that best fits the data should describe the average fissioning species. Because the Halpern and Strutinski work should be most applicable for large excitation energies, it is used in all these discussions. Griffin's theory provides the same final results, but wherever differences occur, they are pointed out.

1. Comparison of the Data with Theory

a. Angular distributions. The theoretical angular distributions from the p and r values in best agreement with the data for 124.6-Mev C^{12} bombardments of bismuth are presented in Fig. 29. A $1/\sin\theta$ reference function is also included in each case to point out the salient differences. In general both theories generate angular distributions that follow the function $1/\sin\theta$ at angles near 90 deg. The primary deviation arises from the manner in which 0 deg is approached. Halpern and Strutinski's results exhibit a definite negative curvature in this region while Griffin's curves behave linearly. It should also be noted that, for the same value of I and K, the latter predictions follow the function $1/\sin\theta$ over a longer interval of angles than the former. In addition, Griffin's functions exceed the value of $1/\sin\theta$ slightly between 30 and 50 deg for large r.

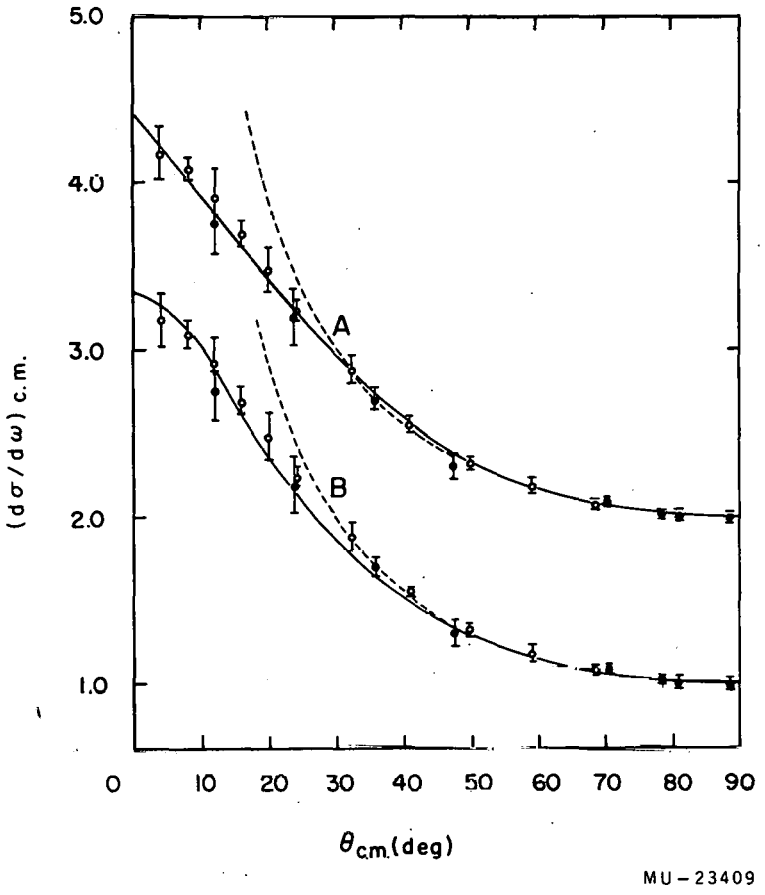

Fig. 29. Center-of-mass angular distribution from 124.6-Mev C^{12} bombardment of Bi^{209}. (A) Theoretical curve for r=3.5 from Griffin; (B) theoretical curve for p=5.3 from Halpern and Strutinski. The dashed curves are functions of $1/\sin\theta$. The differential cross sections at 90^{o} are unity. ⊛ - catcher angle θ; O - catcher angle $\pi - \theta$.

In comparing the theoretical curves with the data, one must remember that the visible angular distribution receives contributions from a large number of individual events. Hence, a single p or r parameter should not necessarily fit the data precisely. The example of Fig. 29 shows the same general features as do the remainder of the center-of-mass comparisons in Figs. 15 through 22. Because of the size of the experimental errors, neither of the two theories can be ruled out. However, from consideration of the several measurements, the following behavior appears consistently. As one goes from 90 deg towards 0 deg, the data behave according to the function $1/\sin\theta$ at first, and then go through an inflection point as 0 deg is approached. Near 0 deg the angular distribution function seems to have a definite negative curvature. As one goes to lower bombarding energies, the distributions break away from the value of $1/\sin\theta$ at angles nearer 90 deg. If one were to attempt to point out any weaknesses in the theories, they would be (a) the Griffin predictions seem inappropriate in their linear approach to 0 deg, and (b) the Halpern and Strutinski functions suffer from being somewhat low in the region 20 to 50 deg.

Referring to Figs. 15 through 22, the choice of p values for the best fit to the data was weighted to emphasize the angles near 0 deg because these describe the anisotropy most accurately. The angular distributions for maximum bombarding energies are also compared with the function $1/\sin\theta$.

b. The function $K_0^2(E^* - E_f)$. In addition to testing the theoretical fits to the angular-distribution data, it is worth while to examine the dependence of K_0^2 on the excitation energy. At high energies this function can be obtained by measurement of angular distributions in which quite fissionable compound nuclei are formed. Here, fission should precede any neutron evaporation so that E^* can be estimated fairly well. If we know $\overline{\ell}$, determination of the anisotropy parameter p as a function of energy permits us to calculate the value of K_0^2 at several excitation energies. In the fission of U^{233} and U^{235} with alpha particles, it has been determined that the average excitation energy

at the fission point is lowered only 4 and 8% respectively due to neutron evaporation.[51] The Z^2/A values for the systems cited above are only slightly greater than those for the compound nuclei formed from bismuth with nitrogen or oxygen. If the angular momentum increases the fissionability, then these latter two cases should provide at least a lower limit for the dependence of K_0^2 on $(E^* - E_f)$. This relationship is shown in Figure 30 along with the Halpern and Strutinski theoretical curve. To illustrate the trends among other ions, similar curves for carbon on both targets are included. The fission-barrier heights were calculated from the formulae of Hiskes,[6] using the values of Thomas for the angular momentum of the compound nucleus.[39] These are listed below in Table II.

Figure 30 indicates that a linear function for $K_0^2(E^* - E_f)$ seems to agree with the data better than the square-root dependence predicted from statistical theory. However, first-order corrections to this result would move the data in the direction of the theoretical curve. Neutron evaporation and incomplete momentum-transfer effects shift the function to lower values of $(E^* - E_f)$. Also, if $\bar{\ell}$ is lower than calculated at high energies, K_0^2 will be lowered. The fact that the nitrogen and oxygen points lie roughly on the same line suggests that a limiting value of $K_0^2(E^* - E_f)$ may have been attained. Further experiments are needed to examine this result more closely. Bombarding bismuth and lead targets with fluorine and neon ions should improve these correlations if the previously discussed discrepancy with full momentum transfer does not become too severe. Selection of a heavier target probably would not help in view of the failure to find full momentum transfer with C^{12} bombardments of uranium, as reported by Gordon et al.[55]

2. The Average Fissioning Nucleus

From the experimental angular distributions we have defined a nucleus that represents the average fission process for each reaction that has been studied. The properties of these species calculated in terms of the Halpern and Strutinski theory are presented in Table II.

Table II. Properties of each target—heavy-ion system and of the average fissioning nucleus

Target	Heavy ion	E_{lab} (Mev)	$\bar{l}$	E^* (Mev)	r	p	K_0^2	E_f (Mev)	E^* at fission[a] (Mev) (1)	(2)	Average fissioning nucleus[a] (1)	(2)	$\bar{n}$ emitted before fission[a] (1)	(2)
Au^{197}	B^{11}	114.3	43.6	105	4.5	8.1	132	12.1	29.5	50.6	$Po^{201.7}$	$Po^{203.6}$	6.3	4.4
	C^{12}	124.6	45.8	101	4.3	7.5	157	10.2	34.6	55.9	$At^{203.6}$	$At^{205.5}$	5.4	3.5
		118.2	43.5	94.7	4.2	7.5	142	10.4	30.5	51.7	$At^{202.9}$	$At^{204.8}$	6.1	4.2
		112.1	41.3	89.0	4.1	7.2	133	10.6	28.1	49.3	$At^{204.0}$	$At^{205.8}$	5.0	3.2
		108.0	39.7	85.1	4.2	7.4	120	10.7	24.7	45.6	$At^{204.0}$	$At^{205.8}$	5.0	3.2
		81.0	27.3	59.7	3.8	5.9	71.1	11.5	22.5	32.2	$At^{205.8}$	$At^{206.7}$	3.2	2.3
		69.9	20.4	49.2	3.4	5.1	45.9	11.9	21.4	25.2	$At^{206.5}$	$At^{206.9}$	2.5	2.1
	N^{14}	145.4	53.6	118	4.1	7.0	231	8.7	62.0	75.9	$Rn^{206.7}$	$Rn^{207.7}$	4.3	3.3
		127.2	46.9	101	4.0	6.5	190	9.4	45.4	64.6	$Rn^{206.6}$	$Rn^{208.0}$	4.4	3.0
		107.0	38.3	82.9	3.7	5.4	153	10.0	33.5	54.5	$Rn^{206.1}$	$Rn^{207.8}$	4.9	3.2
		83.1	24.8	60.8	3.2	4.2	82.4	10.9	22.7	34.9	$Rn^{207.8}$	$Rn^{208.7}$	3.2	2.7
	O^{16}	166.1	61.4	124	4.5	8.5	249	7.1	69.0	79.5	$Fr^{208.7}$	$Fr^{209.6}$	4.3	3.4
		142.9	52.8	103	4.3	7.7	204	8.0	49.6	67.3	$Fr^{208.7}$	$Fr^{210.2}$	4.3	2.8
		116.8	41.1	78.8	4.0	6.4	148	9.1	31.1	52.1	$Fr^{209.0}$	$Fr^{210.5}$	4.0	2.2
		84.3	20.0	49.8	2.9	3.6	62.5	10.1	20.6	28.3	$Fr^{210.5}$	$Fr^{211.2}$	2.5	1.8
Bi^{209}	B^{11}	114.3	43.8	88.2	3.6	5.4	200	9.4	49.4	67.5	$Ra^{216.2}$	$Ra^{218.0}$	3.8	2.0
	C^{12}	124.6	45.7	85.7	3.5	5.4	222	8.3	57.6	72.8	$Ac^{218.4}$	$Ac^{219.8}$	2.6	1.2
		112.1	41.3	73.4	3.4	5.0	192	8.6	45.4	64.4	$Ac^{218.2}$	$Ac^{220.1}$	2.8	0.9
		104.5	38.1	66.2	3.3	4.6	176	8.8	39.7	60.0	$Ac^{218.3}$	$Ac^{220.5}$	2.7	0.5
		97.4	35.1	59.6	3.3	4.5	154	9.0	32.7	52.8	$Ac^{218.2}$	$Ac^{220.4}$	2.8	0.6
		89.7	31.3	52.5	3.1	4.1	134	9.2	27.1	48.2	$Ac^{218.2}$	$Ac^{220.6}$	2.8	0.4
		81.0	26.4	44.3	2.9	3.6	110	9.4	23.4	41.4	$Ac^{218.8}$	$Ac^{220.7}$	2.2	0.3
	N^{14}	145.4	53.5	102	3.4	5.0	322	6.7	108	103	Th^{223}	Th^{223}	0	0
		127.2	46.8	84.8	3.3	4.5	274	7.2	82.2	85.2	$Th^{222.8}$	Th^{223}	0.2	0
		107.0	37.8	65.9	2.9	3.5	230	7.8	60.7	65.4	$Th^{222.4}$	Th^{223}	0.6	0
		83.1	23.6	43.5	2.4	2.6	121	8.6	23.1	43.0	$Th^{221.7}$	$Th^{222.9}$	1.3	0.1
	O^{16}	166.1	61.7	107	3.8	5.9	363	5.4	137	108	Pa^{225}	Pa^{225}	0.4	0
		142.9	52.7	86.0	3.7	5.7	274	6.1	81.1	86.2	$Pa^{224.6}$	Pa^{225}	0	0
		116.8	39.4	61.9	3.4	4.6	190	7.0	43.0	61.1	$Pa^{223.1}$	$Pa^{224.9}$	1.9	0.1
		84.3	14.2	31.7	2.0	1.7	66.7	8.0	18.8	31.6	$Pa^{223.6}$	Pa^{225}	1.4	0

[a]Here (1) refers to the statistical prediction for $K_0^2(E^*-E_f)$, and
(2) refers to the linear fit to the data from N^{14} and O^{16} bombardments of bismuth.

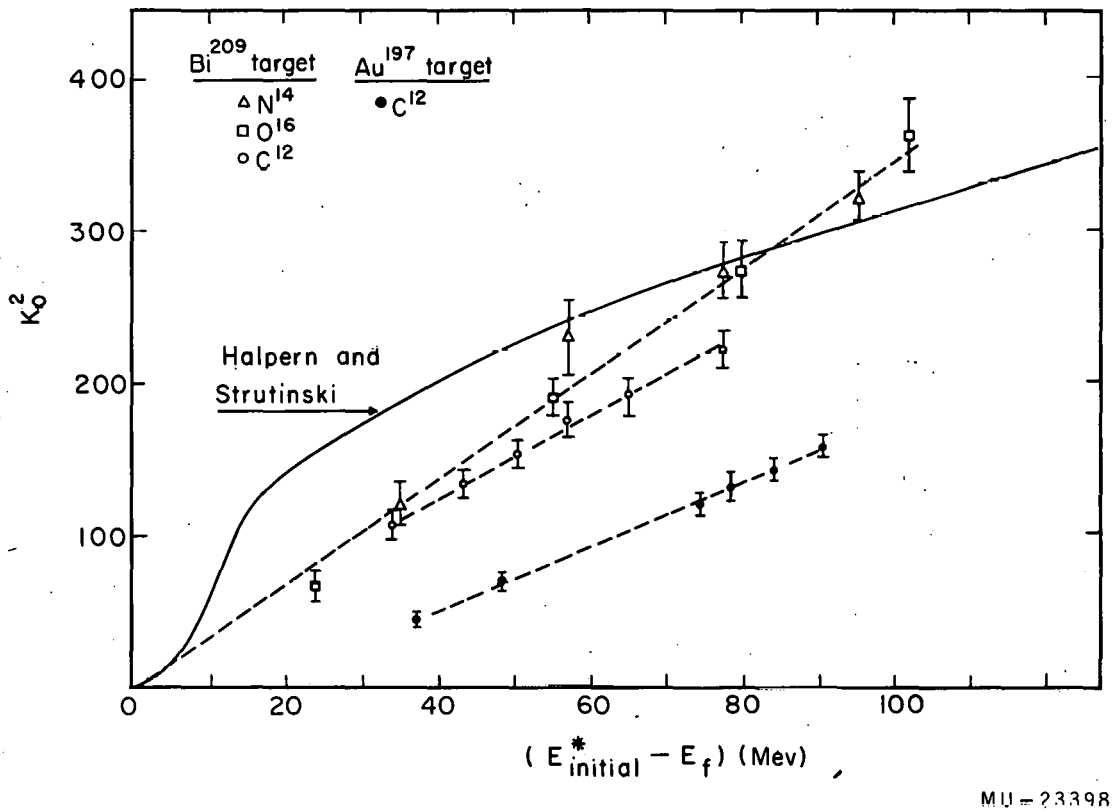

Fig. 30. The value of $K_0^2 = I_{max}^2/4p$ versus $(E^*_{initial} - E_f)$ of the initial compound nucleus. The solid curve is the theoretical prediction of Halpern and Strutinski: dashed curves represent the experimental data.

The average angular momentum, excitation energy, fission barriers, and p and r were determined as previously stated. The value of K_0^2 was fixed from the relationship $K_0^2 = I_{max}^2/4p$, on the assumption that $\overline{I} = \overline{\Gamma} = (2/3)I_{max}$ and that $\overline{\Gamma}$ remains constant up to the point of fission. The average value of $(E^* - E_f)$ was extracted from the theory for the two extreme dependencies of K_0^2 on excitation energy; i.e. (a) from Halpern and Strutinski's theoretical curve, and (b) from the empirical curve based on the N^{14} and O^{16} bombardments of bismuth.

The difference between the initial excitation energy of the compound nucleus and the same quantity at the point of fission was presumed to have been dissipated in neutron evaporation. The neutron binding energies of Cameron[39] and appropriate assumptions about the average energy of an evaporated neutron were then used to determine the average fissioning nucleus. It should be pointed out that nuclei of lower Z should also be included here. However, the large total neutron cross sections (10 barns) reported by Hubbard et al. for related reactions[56] compared with the alpha-particle and proton evaporation cross sections (100 to 300 mb) of Britt and Quinton,[53] indicate that neutron emission is the primary mode of de-excitation. Furthermore, the fission probabilities for these lower-Z states should be somewhat smaller.

Because of the many assumptions involved, these calculations should be interpreted cautiously, particularly when one observes the differences resulting from the two extreme dependencies of K_0^2 on the excitation energy. However, these numerical estimates present a general picture that is consistent with our discussions of Γ_f/Γ_n for $Z < 90$. For $Z = 90$ and 91, the calculations indicate that nearly all the fission events occur before neutron evaporation, as would be expected for these elements.

For $Z < 90$ the most obvious correlation that can be drawn from Table II is the increase in Γ_f/Γ_n for nuclei of progressively higher Z. This result is substantiated in part by Latimer's measurements of the cross sections for neutron-evaporation products.[41] At a given excitation energy, the astatine isotope produced in greatest abundance

(50 to 100 mb) is usually about one mass unit lighter than the average fissioning nucleus estimated from considerations of the statistical theory. This fact additionally suggests that Γ_f/Γ_n is probably decreasing rapidly at low excitation energies. Britt and Quinton have found that with the same heavy ion, the alpha-particle evaporation yields are about twice as large for gold as for bismuth targets, although the fission cross section is larger for the latter case. This result further supports the argument that more excitation energy is dissipated in particle evaporation as Z of the compound nucleus decreases.

If we consider the nuclei near Z = 85, the theoretical treatment of the data reveals that, on the average, several neutrons must be emitted before fission in order to explain the anisotropy that is observed. At the same time, measurements of the total fission cross sections report that the level width for fission remains quite large in this region.[23] Hence, it appears that Γ_n/Γ_f must be an increasing function of the excitation energy or a decreasing function of the mass of the compound nucleus (or, more probably, both). This statement is consistent with the form of the expression for Γ_n/Γ_f proposed by Fujimoto and Yamaguchi,

$$\Gamma_n/\Gamma_f \propto T \exp(E_f - B_n)/T \qquad (13)$$

where the nucler temperature, T , equals $(10E^*/A)^{1/2}$, and B_n is the neutron binding energy.[57]

It may well be that the effect of angular momentum is to increase the level width for fission as predicted by Pik-Pichak. However, according to Ericson and Strutinski, at high excitation energies there is a high density of states that can be populated by neutron evaporation. Thus, it appears that the level width for neutron emission may increase more rapidly than that for fission when the excitation energy is large. The alternative to this conclusion would be that the theory needs to be re-evaluated for heavy-ion-induced fission reactions. Studies of the angular distributions from less fissionable systems should provide a good test for the above interpretations.

V. SUMMARY

The angular distributions from fission induced by heavy ions can be characterized in the following manner.

(a) The fission fragments are emitted preferentially in the forward and backward direction with respect to the beam axis.

(b) As the bombarding energy increases, the anisotropy increases. This rise is qualitatively related to the ratio of the average angular momentum for the reaction to the excitation energy of the compound nucleus.

(c) For the same bombarding particle, the anisotropy decreases as the value of Z^2/A for the compound nucleus becomes larger. The above observations agree with the findings from fission induced by lighter particles at lower energies.

(d) In contrast to the low-energy results, no clear-cut monotonic relationship is evident between the mass of the projectile and the anisotropy. Angular distributions of fission fragments obtained with N^{14} as the incident particle are anomalously lower than those obtained from C^{12} and O^{16} bombardments. This effect becomes less important as the bombarding energy decreases, but is only tentatively explained.

In general the experimental results can be adequately described by the theoretical predictions of Halpern and Strutinski and of Griffin for fission at moderate energies. Interpretation of the data in the framework of these theories suggests:

(a) The value of Γ_n/Γ_f decreases as Z of the compound nucleus becomes larger.

(b) At an excitation energy above 40 to 50 Mev, Γ_n/Γ_f may increase substantially with increasing excitation energy and (or) decreasing mass of the compound nucleus.

There is also some evidence that the distribution of fission-channel quantum numbers may be a linear function of the excitation energy rather than obeying a square-root dependence, as predicted by statistical theory.

ACKNOWLEDGMENTS

I wish to thank my research director, Professor Glenn T. Seaborg, for his guidance and interest in this work.

I am sincerely indebted to Drs. T. Darrah Thomas and John Alexander for their continued encouragement and for their many valuable suggestions concerning both the experimental procedures and treatment of results.

For their many helpful discussions of this work I thank Drs. H. M. Blann, Glen E. Gordon, Torbjørn Sikkeland, and John Gilmore, and Messrs. Bruce Wilkins, Lawrence Altman, and Robert M. Latimer. I also am grateful to Drs. John D. Axe and Denis McWahn, and Messrs. Eldon Haines, Lee Hyder, Paul Reeder, and Richard Kiefer for many stimulating discourses in the fields of nuclear and heavy-element chemistry.

Discussion of these results with Drs. John O. Rasmussen, John R. Huizenga, and William Knox were very enlightening.

The cooperation of Mr. Albert Ghiorso and Dr. E. L. Hubbard in permitting me to use the experimental facilities at the Hilac is greatly appreciated. My sincere thanks go to Messrs. James Johnston, Ross Grazier, and Norman Stewart of the Hilac electronics-maintenance staff for development of the counting system and for maintaining it in excellent operating condition. The assistance of the Hilac crew consisting of Messrs. Chester Hatch, Donald F. Lebeck, Wilfred P. Kimlinger, Robert H. Burkett, Harold L. Vyverberg, Douglass McHugh, Edward Jenkins, and Thomas E. Bowman was greatly appreciated.

I am grateful to Mr. Charles A. Corum for his design of the apparatus and to Mr. Daniel G. O'Connell for the preparation of the targets.

I wish to thank Marthamae Snyder, the Graphic Arts Department, and the Information Division for assistance with the preparation of this thesis.

I am indebted to the University of California and the Woodrow Wilson Science Foundation for providing me with fellowships during this research.

This work was performed under the auspices of the U.S. Atomic Energy Commission.

APPENDICES

A. Kinetic Energy of the Fission Fragments

An indirect measurement of the average kinetic energy of the fission fragments is obtained as a by-product of the angular-distribution experiments. If it is assumed (a) that the transfer of momentum from the projectile to the compound nucleus is complete, and (b) that only binary fission occurs, then from Eq. (5) the average c.m. kinetic energy for the fission fragments is

$$\bar{E}_{c.m.} = \frac{M_p \bar{E}_p M_f}{M_{CN}^2 \bar{\eta}^2} \quad . \tag{5}$$

The mass and energy of the projectile (M_p and E_p) and of the initial compound nucleus (M_{CN} and $M_p E_p / M_{CN}$) are known. By determining $\bar{\eta}$ as has been done in Section IIIB, only the mass of the average fission fragment M_f, is needed to calculate the corresponding kinetic energy.

The corrections to the above formula arising from light-particle evaporation are minor. To a good approximation, the velocity of the compound nucleus remains constant during such processes. Therefore, changes in the mass of the compound nucleus will be directly balanced by the lowering of its kinetic energy required to conserve momentum. The conservation of momentum perpendicular to the beam direction also insures that the deviation in angle of the compound nucleus from its original path, ϕ, will be quite small:

$$\sin \phi_{max} = (M/M_{CN})^{1/2} \quad ,$$

where M represents the mass of the evaporated particle. Any post-fission neutrons that are emitted can only serve to smear out the angular distribution, thus lowering $\bar{\eta}$ slightly. However, if these neutrons are emitted isotropically, this source of error should be negligible.

The primary uncertainty in the calculation of $\bar{E}_{c.m.}$ is the average mass of the fission fragments. In Table III the c.m. kinetic energy

Table III. Average kinetic energy of the fission fragments.

		Au^{197} target				Bi^{209} target			
Heavy ion	E_{lab}	E_1[a]	E_2[b]	E_3[c]	Error	E_1[a]	E_2[b]	E_3[c]	Error
B^{11}	114.3	72.7	71.2	70.5	± 4	77.6	76.9	76.3	± 4
C^{12}	124.6	73.9	72.7	72.0	± 4	81.3	80.9	80.3	± 4
	118.2	72.1	70.7	70.0	± 4	-	-	-	-
	112.1	72.3	71.2	70.6	± 5	78.5	78.2	77.5	± 5
	108.0	72.4	71.3	70.7	± 5	-	-	-	-
	104.5	-	-	-	-	78.6	78.4	77.6	± 4
	97.4	-	-	-	-	78.1	77.9	77.1	± 6
	89.7	-	-	-	-	75.2	75.1	74.2	± 6
	81.0	70.2	69.4	69.1	± 5	75.3	75.2	74.6	± 6
	69.9	69.5	68.8	68.7	± 5	-	-	-	-
N^{14}	145.4	76.6	75.4	75.0	± 4	(84.8)	(84.8)	(84.8)	+4, -7
	127.2	72.7	71.7	71.2	± 5	81.8	81.8	81.8	± 4
	107.0	72.6	71.5	70.9	± 6	77.7	77.7	77.5	± 5
	83.1	73.2	72.4	72.1	± 6	77.9	77.9	77.5	± 6
O^{16}	166.1	76.3	75.1	74.8	± 5	(89.4)	(89.4)	(89.4)	+4,-8
	142.9	74.7	73.7	73.2	± 6	(87.4)	(87.4)	(87.2)	+4, -8
	116.8	76.1	75.3	74.6	± 4	(86.6)	(86.6)	(85.9)	+5,-9
	84.3	73.6	73.0	72.7	± 5	80.5	80.5	80.0	±5

[a]Here $E_1 - M_f$ is one-half of the fissioning compound nucleus.

[b]Here $E_2 - M_f$ is one-half the mass of the fissioning compound nucleus calculated from linear dependence of K_0^2 on $(E^* - E_f)$.

[c]Here $E_3 - M_f$ is one-half the mass of the fissioning compound nucleus calculated from statistical dependence of K_0^2 on $(E^* - E_f)$.

has been calculated for three assumed masses corresponding to symmetric division of the original compound nucleus and the two average fissioning nuclei calculated in Table II. The limits of error arise from uncertainties in $\bar{\eta}$ only.

In general, the results listed in Table III agree quite well with the direct measurements of the fragment kinetic energies.[19,20] The exception to this is the case of the Bi^{209} (O^{16}, f) reactions, where is has been suggested that the momentum transfer is about 5% low. Whenever a substantial disagreement with full momentum transfer is found, the calculated results are enclosed in parentheses.

Although the limits of error prevent any conclusive analysis of these data, it appears that the kinetic energy may increase slightly with greater bombarding energy. This effect presumably could be a manifestation of the excitation energy of the nucleus at the time of fission. The data are roughly in accord with the dependence of the kinetic-energy release in fission on $Z^2/A^{1/3}$ predicted by Terrell.[58]

B. Calculation of a Representative Angular Distribution

The proper form for the application of the theory to the data has been discussed in Section IVC. Because the compound system formed from carbon and gold has been studied in some detail, it was felt that one could attempt a more thorough analysis of this information. It should be stressed that the level width ratios for the various de-excitation processes involved here are not known. Consequently, these quantities are used as parameters to provide the best correlation between the observed cross sections, the angular distribution, and conservation of energy. Attempts to utilize some form of Eq. 13 for Γ_n/Γ_f met with little success because of uncertainties in the absolute magnitude of the fission barriers.

The compound-nucleus At^{209} formed from bombardment of Au^{197} with 81.0-MevC^{12} ions was chosen for this analysis. At this comparatively low excitation energy, charged particle emission should be minimized, and there should be fewer available neutron-evaporation

stages. The following data for this system has been used here:

(a) fission cross section: $\sigma_f = 400$ mb; from Gordon et al.[19]

(b) spallation cross sections:

$$\left.\begin{aligned} \sigma(C^{12}, 4n) &\cong 10 \text{ mb} \\ \sigma(C^{12}, 5n) &\cong 65 \text{ mb} \\ \sigma(C^{12}, 6n) &\cong 15 \text{ mb} \end{aligned}\right\} \text{; from Latimer}[41]$$

$$\left.\begin{aligned} \sigma_a &\leq 25 \text{ mb} \\ \sigma_p &\leq 50 \text{ mb} \end{aligned}\right\} \text{; estimated from Britt and Quinton}[53]$$

(c) $p = 5.9$; this work.

To determine the various fissioning species, it was assumed that all charged-particle emission took place from the initial compound nucleus. The average excitation of each resulting state was then calculated from Cameron's mass tables and the relationship

$$\Delta E = B_n + 2T.$$

To first order, this discrete set of energies should be a good approximation to the broadened excitation-energy spectrum which results from the energy distribution of the evaporated particles.

The total angular momentum was assumed to be constant throughout all de-excitation processes and to be equal to the value of $\bar{\ell}$ calculated by Thomas. The fission barriers were calculated from the predictions of Hiskes by using the above value of the average angular momentum. These properties of the fissioning species are summarized in Table IV along with the anisotropy parameter p calculated from the linear function for $K_0^2(E^* - E_f)$ of Section IVC1. It was found that use of the statistical prediction for this function imposed severe limitations on the values of Γ_f/Γ_n; specifically, nearly all of the fission would have been forced to occur at excitation energies within about 10 Mev of the fission barrier. Although such behavior is conceivable, it does not seem likely that Γ_f/Γ_n should undergo such a drastic change in this energy region (10 to 60 Mev).

Table IV. Properties of various assumed stages of fission used to provide theoretical fit to data for 81.0-Mev C^{12} bombardment of Au^{147}.

Compound nucleus	k	E^* (Mev)	E_f (Mev)	E^*-E_f (Mev)	p_{linear}	Assumed Γ_n/Γ_f	Assumed Γ_p/Γ_f	Assumed Γ_α/Γ_f
At^{209}	1	59.7	11.9	47.8	2.56	(11)	(1.4)	(0.7)
At^{208}	2	47.5	11.5	36.0	3.39	(6.0)		
At^{207}	3	36.9	11.1	25.8	4.77	(1.4)		
At^{206}	4	24.5	10.8	13.7	9.55	(1.2)		
At^{205}	5	14.5	10.5	4.0	30.0	(4.0)		
Po^{208}	6	48.0	14.2	33.8	3.62	(11)		
Po^{207}	7	36.4	13.8	22.6	5.38	(1.3)		
Po^{206}	8	26.3	13.4	12.9	10.0	(0.6)		
Bi^{205}	9	38.1	15.1	23.0	5.32	(2.1)		
Bi^{204}	10	26.0	14.7	11.3	10.9	(1.4)		

From these semi-quantitative considerations and Eq. (12), the angular distribution can be described by the function

$$W(\theta) = 0.09p_1 + 0.143p_2 + 0.35p_3 + 0.23p_4 + 0.05(p_5 + p_7)$$
$$+ 0.01p_6 + 0.04p_8 + 0.02p_9 + 0.017p_{10},$$

where p_k refers to the value of the anisotropy parameter p at the angle θ for the compound nucleus k. This fit to the data is shown in Fig. 31. The features of $W(\theta)$ are quite similar to those of individual p curves. However, the composite angular distribution has a steeper slope near 0 deg. than does the corresponding function for a single p value. It is also observed that there is no set of p's that will give a good fit to the data points near 0 and 30 deg at the same time.

Although this treatment has been somewhat superficial, it illustrates the complexity of fission reactions induced by heavy ions. The results of the calculation regarding the best values for Γ_f/Γ_n also serve to emphasize the conclusions of Section IVC in greater detail, i.e. Γ_f/Γ_n appears to decrease at high excitation energies and (or) lower A of the compound nucleus.

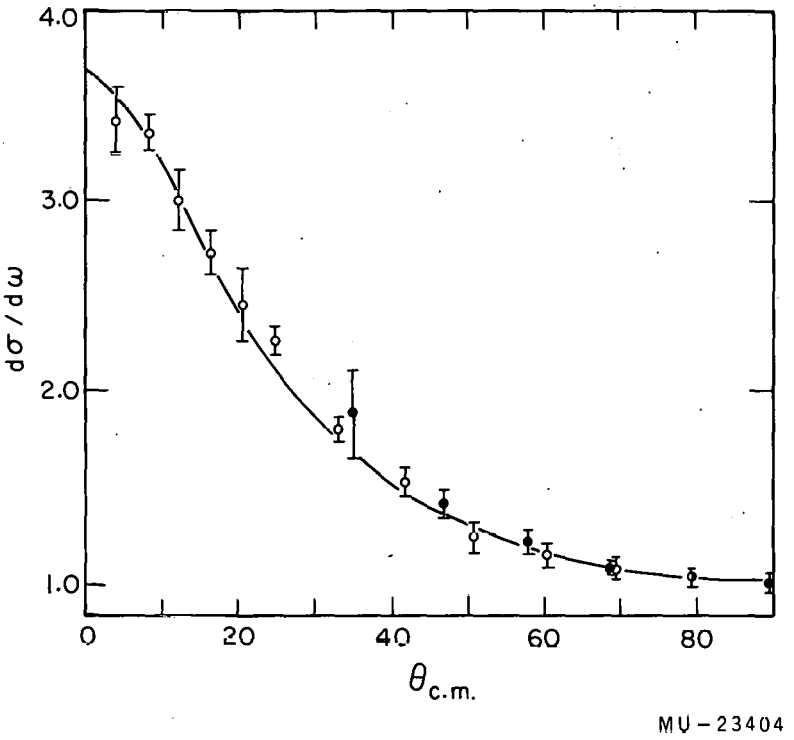

Fig. 31. Center-of-mass data from 81.0-Mev C^{12} on Au^{197} fitted with composite angular distribution from assumed stages of the de-excitation process.

REFERENCES

1. A. Zucker, in Annual Reviews of Nuclear Science, Vol. 10 (Annual Reviews, Inc., Palo Alto, California, 1960), p 27.
2. N. Bohr and J. A. Wheeler, Phys. Rev. 56, 426 (1939).
3. J. Frankel, Phys. Rev. 55, 987 (1939).
4. W. J. Swiatecki, Proceedings of the Second United Nations Conference on the Peaceful Uses of Atomic Energy, Vol. 15 (United Nations, Geneva, 1958), p. 248.
5. G. A. Pik-Pichak, Soviet Phys. JETP 7, 238 (1958).
6. John R. Hiskes, The Liquid Drop Model of Fission; Equilibrium Configurations and Energetics of Uniform Rotating Charged Drops (Thesis), Part I, UCRL-9275, June 16, 1960.
7. E. J. Winhold, P. T. Demos, and I. Halpern, Phys. Rev. 85, 728 (A) (1952).
8. J. E. Brolley and W. C. Dickinson, Phys. Rev. 94, 640 (1954).
9. J. E. Brolley, W. C. Dickinson, and R. L. Henkel, Phys. Rev. 99, 159 (1955).
10. B. L. Cohen, W. H. Jones, G. H. McCormick, and B. L. Ferrell, Phys. Rev. 94, 625 (1954).
11. I. Halpern and C. T. Coffin, Phys. Rev. 112, 536 (1958).
12. E. K. Hyde, A Review of Nuclear Fission, Part I. Fission Phenomena at Low Energy, UCRL-9036; January 1960; Part II Fission Phenomena at Moderate and High Energies, UCRL-9065, February 1960; part II, p. 77, (to be published).
13. I. Halpern, in Annual Reviews of Nuclear Science, Vol. 9 (Annual Reviews, Inc., Palo Alto, California, 1959), p. 245.
14. R. B. Leachman, Proceedings of the Second United Nations International Conference on the Peaceful Uses of Atomic Energy, Vol. 15 (United Nations, Geneva, 1958), p 229.
15. J. R. Huizenga, Nuclear Reactions, Vol. II (North-Holland Publishing Co., Amsterdam, in press).

16. A. Bohr, Proceedings of the International Conference on the Peaceful Uses of Atomic Energy, Vol. 2 (United Nations, New York, 1956), p. 151.
17. I. Halpern and V. Strutinski, Proceedings of the Second United Nations International Conference on the Peaceful Uses of Atomic Energy, Vol. 15, (United Nations, Geneva, 1958), p.400.
18. J. J. Griffin, Phys. Rev. 116, 107 (1959).
19. G. E. Gordon, A. E. Larsh, T. Sikkeland, and G. T. Seaborg, Phys. Rev. 120, 1341 (1960).
20. H. C. Britt and A. R. Quinton, Phys. Rev. 120, 1768 (1960).
21. E. Goldberg, H. L. Reynolds, and D. D. Kerlee, Proceedings of the Second Conference on Reactions Between Complex Nuclei (John Wiley and Sons, Inc., New York, 1960), p. 230.
22. V. E. Viola, H. M. Blann, and T. D. Thomas, ibid., p. 224.
23. J. Gilmore, The Effect of Angular Momentum on Fission Probability (thesis), UCRL-9304, July 1960.
24. A. W. Fairhall, R. C. Jensen, and E. F. Neuzil, Proceedings of the Second United Nations International Conference on the Peaceful Uses of Atomic Energy, Vol. 15 (United Nations, Geneva, 1958), p.452.
25. Torbjørn Sikkeland, Lawrence Radiation Laboratory, private communication.
26. L. C. Northcliffe, Phys. Rev. 120, 1744 (1960).
27. R. M. Sternheimer, Phys. Rev. 115, 137 (1959).
28. Edward L. Hubbard, Range-Energy Relation for Heavy Ions in Metals, UCRL-9053, January 25, 1960.
29. J. M. Alexander and M. F. Gazdik, Phys. Rev. 120, 874 (1960).
30. Glen E. Gordon, Fission and Spallation in Nuclear Reactions Induced by Heavy Ions(thesis), UCRL-9083, May 1960 Appendix A.
31. C. T. Coffin, Angular Distributions in Fission Produced by Alpha Particles and Deuterons, (thesis), University of Washington, 1956.
32. J. M. Alexander and L. Winsberg, Phys. Rev. 121, 518, 529 (1961).

33. E. L. Hubbard and G. Merkel, Proceedings of the Second Conference on Reactions between Complex Nuclei (John Wiley and Sons, Inc., New York, 1960), p. 25.
34. H. M. Blann, Fission of Gold with 112-Mev C^{12} Ions: A Yield-Mass and Charge Distribution Study, (thesis), UCRL-9190 May 23, 1960.
35. L. A. Altman, Lawrence Radiation Laboratory, private communication.
36. J. B. Marion, T. I. Arnette, and H. C. Owens, Tables for the Transformation between the Laboratory and Center-of-Mass Coordinate System and for Calculation of the Energies of Reaction Products, Oak Ridge National Laboratory Report ORNL-2574, April 1959.
37. E. Haines, Lawrence Radiation Laboratory, private communication.
38. T. D. Thomas, Phys. Rev. 116, 703 (1958).
39. A. G. W. Cameron, A Revised Semi-Empirical Atomic Mass Formula, Chalk River Report CRP-690, March 1957.
40. D. S. Burnett and S. G. Thompson, Fission Thresholds for Elements Lighter than Radium, UCRL-9321, July 25, 1960.
41. Robert M. Latimer, Lawrence Radiation Laboratory, unpublished results.
42. J. E. Simons and R. L. Henkel, Bull. Am. Phys. Soc. (II) 4, 233, 373 (1959).
43. L. Blumberg and R. B. Leachman, Phys. Rev. 116, 102 (1959).
44. E. P. Wigner, Proceedings of the Second Conference on Reactions Between Complex Nuclei (John Wiley and Sons, Inc., New York, 1960), p. 305.
45. A. W. Fairhall, I. Halpern, and E. J. Winhold, Phys. Rev. 94, 733 (1954).
46. B. L. Cohen, W. H. Jones, G. H. McCormick and B. L. Ferrell, Phys. Rev. 94, 625 (1954).
47. M. Hickenlooper, Annual Progress Report, University of Washington Cyclotron, 1956.

48. T. Ericson and V. Strutinski, Nuclear Physics 8, 284 (1958).
49. T. Darrah Thomas, Brookhaven National Laboratory, private communication.
50. H. G. Hicks and R. S. Gilbert, Phys. Rev. 100, 1286 (1955).
51. R. Vandenbosch, T. D. Thomas, S. E. Vandenbosch, R. A. Glass and G. T. Seaborg, Phys. Rev. 111, 1358 (1958).
52. R. Kauffman and R. Wolfgang, Phys. Rev. 121, 192 (1961).
53. H. C. Britt and A. R. Quinton, Phys. Rev. Letters, to be published.
54. A. E. Larsh, G. E. Gordon, T. Sikkeland, and J. R. Walton, Proceedings of the Second Conference on Reactions Between Complex Nuclei, (John Wiley and Sons, Inc., New York 1960), p.208.
55. G. A. Pik-Pichak, Soviet Physics: JETP 9, 679L (1959).
56. E. Hubbard, R. Main and R. Pyle, Phys. Rev. 118, 507 (1960).
57. Y. Fujimoto and Y. Yamaguchi, Prog. Theoret. Phys. 5, 76 (1950).
58. J. Terrell, Phys. Rev. 113, 527 (1959).